CHAPTER 1

Development of the Heart and Great Vessels

Peter J. Gruber,[1] Andy Wessels,[2] and Steven W. Kubalak[2]

[1]Primary Children's Medical Center, Salt Lake City, UT, USA
[2]Medical University of South Carolina, Charleston, SC, USA

Introduction

Modern cardiac embryology combines molecular and cellular biologic techniques with traditional embryologic morphologic approaches during development. The limited descriptions of human cardiac development are necessarily supplemented by nonhuman models of cardiac development. Avian embryos have traditionally been favored experimental models because of the ease with which they can be observed and manipulated. More recently, the developing mouse has become the preferred model for studying cardiac development because of the strength of genetic and molecular investigative tools available in this species. Where possible, this chapter discusses how results in experimental animal models relate to human cardiac development. Table 1.1 provides a simplified comparison of two widely utilized developmental schemes for developmental staging in chick and mouse embryos [1–7]. The comparison of multiple species provides an important platform for understanding the development of the human heart and the pathogenesis of human disease.

Formation of Cardiac Precursors

All of the cells that will become part of the heart derive from populations of undifferentiated precursors that will be influenced by external signals into their final developmental pathways. In addition to the intellectual challenge of understanding how these acts of differentiation occur, intense activity in this field is also driven by the possibility of controlling cardiac tissue differentiation to replace diseased myocardium in the postnatal heart.

Repeated cell divisions of the fertilized egg form a cell mass that evolves into two distinct layers of cells. The epiblast layer is separated from a second layer of cells, called the hypoblast in the chick or the primitive endoderm in the mouse and human. The next critical stage of development is gastrulation where widespread cell migration into and reorganization within the blastocoele cavity result in the formation of three germ layers (ectoderm, mesoderm, and endoderm) and the determination of the future body plan of the embryo (Figure 1.1) [7,8].

Gastrulation of precardiac cells is an early event in all species. In the human, gastrulation takes place at the beginning of the third week of development and angioblasts in the cardiogenic region are present shortly thereafter. At the time that precardiac cells gastrulate in chick embryos (Hamburger–Hamilton stage 3), the primitive streak is less than 1 mm in length; the portion of the streak through which the precardiac cells ingress extends as a relatively broad swath 0.125–0.75 mm from the anterior limit of the streak [9]. The most anteriorly gastrulating cells contribute to the most anterior portion of the primitive heart tube.

After cells have undergone gastrulation they enter the undifferentiated mesenchyme. Uncommitted precardiac cells enter the primitive streak only to become specified to their cell type or migratory pathways in the mesoderm after leaving the streak [9]. Subsequently, the precardiac cells will move laterally to join the lateral plate mesoderm at the level of Hensen's node. The lateral plate mesoderm then splits into two layers, a splanchnic layer directly above the endoderm and a somatic layer directly below the ectoderm. The anterior endoderm provides signals to splanchnic mesodermal cells to enter the precardiac lineage. Fibroblast growth factors (FGFs)-1, -2, and -4 and bone morphogenetic protein 2 (BMP-2) are proteins that appear to be critical to this process [10]. However, to date no single gene has been identified whose ablation leads to a specific failure of all myocardial differentiation from precardiac mesoderm. This observation may argue the presence of either a considerable genetic redundancy in precardiac myocyte differentiation or an unsuspected diversity of

Pediatric Cardiac Surgery, Fourth Edition. Edited by Constantine Mavroudis and Carl L. Backer.

Table 1.1 Simplified comparison of developmental stages between human, mouse, and chicken embryos.

Human			Mouse	Chicken
Carnegie stage[a]	Streeter horizon[b]	Days gestation	Embryonic days/ (Theiler's stage)[c]	Hamburger/Hamilton stage[d]/(days of incubation)
9	IX	20	8–8.5 (12)	7–8 (1.1)
10	X	22	8.5–9 (13)	10 (1.5)
11	XI	24	9–9.5 (14)	11 (1.8)
12	XII	26	9.5–10.25 (15)	14 (2.2)
13	XIII	28	10.25–10.5 (16)	17 (2.6)
14	XIV–XV	32	10.5–10.75 (17)	19 (2.9)
15	XVI	33	11 (18)	20-21 (3.3)
16	XVIII	37	11.5 (19)	24 (4)
17	XX	41	12 (20)	26 (4.8)
18	XXI–XXII	44	12.5 (21)	28 (5.6)
19	XXIII	47	13 (21)	29–30 (6.4)
20		50	14 (22)	31–32 (7.2)
21		52	14 (22)	34 (8)
22		54	14 (22)	35 (8.7)
23		56	14 (22)	36 (9.6)

[a]O'Rahilly R, Muller F, Streeter GL. (1987) Developmental Stages in Human Embryos. Washington, DC: Carnegie Institution of Washington [2].
[b]Streeter GL. (1942) Developmental horizons in human embryos. Description of age group XI, 13–20 somites, and age group XII, 21–29 somites. Contrib Embryol 30, 211–245 [3]; Streeter GL. (1945) Developmental horizons in human embryos. Description of age group XIII, embryos about 4 or 5 millimeters long, and age group XIV, period of indentation of lens cesicle. Contrib Embryol 32, 27–63 [4]; Streeter GL. (1948) Developmental horizons in human embryos. Description of age group XI, 13–20 somites, age group XV, XVI, XVII, and XVII. Contrib Embryol 32, 133–203 [5].
[c]Theiler K. (1989) *The House Mouse: Atlas of Embryonic Development*. New York, NY: Springer Verlag [6].
[d]Hamburger V, Hamilton HL. (1992) A series of normal stages in the development of the chick embryo. 1951. Dev Dyn 195, 231–272 [1].

precardiac myocyte lineages following independent genetic pathways.

Precardiac cells are found in an epithelial sheet at the cranial end of the splanchnic mesoderm and can be identified at this point by a variety of molecular markers such as the transcription factors NKX2-5, MEF2, HAND1, HAND2, GATA4, TBX5, and ISL1 [11–17]. The region of splanchnic mesoderm expressing precardiac markers is also known as the "heart-forming field" and is larger than the region that will actually contribute cells to the heart tube [18]. In rodent embryos, but not chick embryos, precardiac mesodermal cells exhibit spontaneous contractile activity, indicating a relatively advanced state of differentiation towards the cardiac myocyte lineage [19,20].

The precardiac mesodermal cell mass migrates as a single unit rather than as a collection of independent cells. The precardiac mesodermal sheets on each side of the embryo migrate together towards the midline cranial to the anterior intestinal portal. When the most cranial portions of the bilateral precardiac mesoderm masses meet in the midline, the total premyocardial cell population forms a horseshoe-shaped crescent called the first (primary) heart field. The cues that enable and promote movement of these cells are provided by a noncardiac tissue, the endoderm, as demonstrated by experimental removal of the endoderm and/or ectoderm. The extracellular matrix molecule fibronectin may be one of the important components of the endodermal surface to which the precardiac cells are responding [21].

Precursors of the endocardium follow similar migratory pathways as the precardiac cells, but there are important differences. Pre-endocardial cells and pre-endothelial cells are known as angioblasts. The endocardial angioblasts are first detectable in the splanchnic mesoderm. Mesodermal cells are induced to enter the angioblast lineage by signals such as transforming growth factor beta (TGFβ) 2–4 and vascular endothelial growth factor (VEGF) signaling from the endoderm [10]. Endocardial angioblasts migrate anteriorly and to the midline with the premyocardial cell mass, but they do so as individual cells.

Formation of the Tube Heart

As the precardiac cell masses of the first heart field move steadily towards the midline, endocardial cells begin to

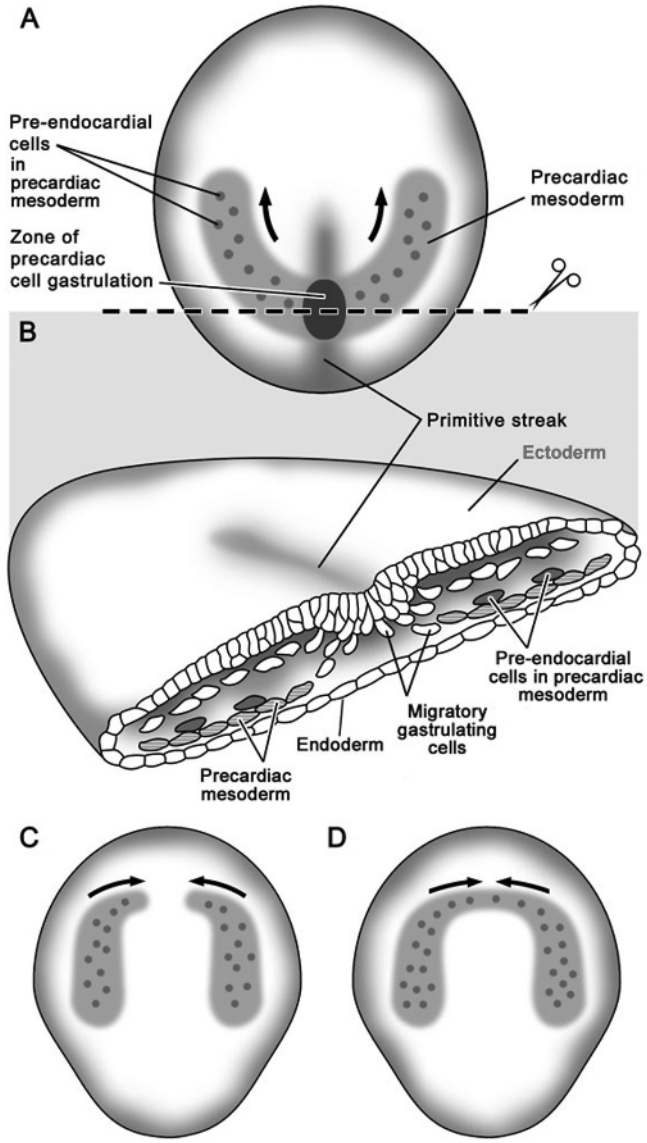

Figure 1.1 Simplified schema of gastrulation, precardiac cell migration, and formation of the heart forming fields. **A,** Cells destined to become cardiac cells migrate from the epiblast into the primitive streak through a broad region caudal to the most anterior portion of the primitive streak. The direction of migration of the gastrulated cells, as indicated by the arrows, is away from the midline and anteriorly on each side. **B,** The embryo in cross-section at the level indicated by the dotted line in **A**. The precardiac mesoderm forms an epithelial sheet closely associated with the endoderm. The pre-endocardial cells are scattered throughout the same region and can be distinguished immunohistochemically from the general precardiac mesoderm. **C,** and **D,** The two lateral precardiac mesoderm populations (also known as heart forming fields) will migrate anteriorly before turning towards the midline (**C**). They will meet in the midline, as shown in **D**, at a location immediately anterior to the anterior intestinal portal.

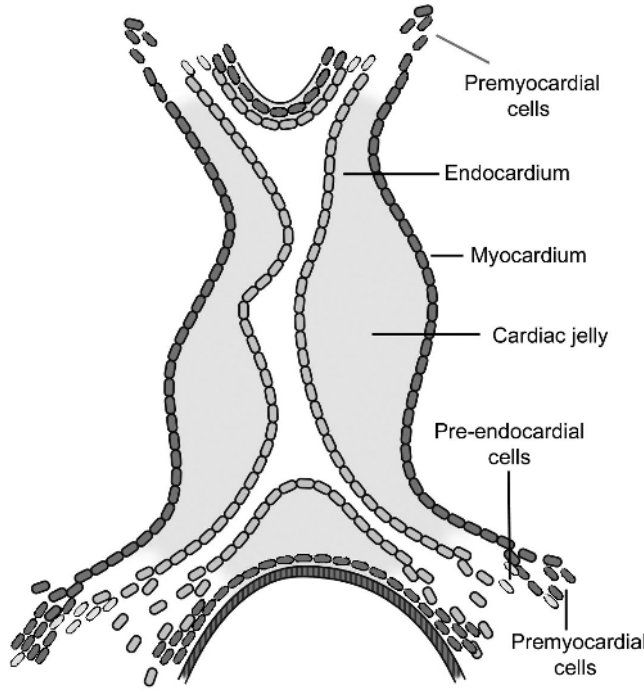

Figure 1.2 Formation of the tube heart is initiated by fusion of the bilateral precardiac mesoderm populations in the midline, resulting in formation of a myocardial tube surrounding an endothelial (endocardial) channel. The myocardial population of the cardiac tube at this stage consists of only the precursors of the future trabeculated portions of the left ventricle. Additional segments are added by ongoing migration of precardiac mesoderm into the tube heart.

form a network of tiny channels that will coalesce into a complex endocardial network surrounded by a myocardial mantle [22]. If the mesodermal sheets are prevented from meeting in the midline as a consequence of genetic [15] or mechanical manipulation [23], dual heart tubes will be formed that undergo some degree of further independent development. However, in normal development, the endothelial network quickly transforms into a single endothelial channel within a single myocardial tube (Figure 1.2) [7].

The tube heart at the time of its formation is connected to the foregut along its dorsal surface throughout its length by a structure called the dorsal mesocardium [24]. As looping proceeds, the dorsal mesocardium degenerates until it remains connected only at the atrial and arterial poles of the heart. The disintegration of the central portion of the dorsal mesocardium is a key event for looping to proceed normally, while the arterial and venous attachments provide "anchors" for the looping heart tube. The mesenchymal portion of the dorsal mesocardium known as the dorsal mesenchymal protrusion [25,26] protrudes into the atrium posteriorly and is a derivative of the second

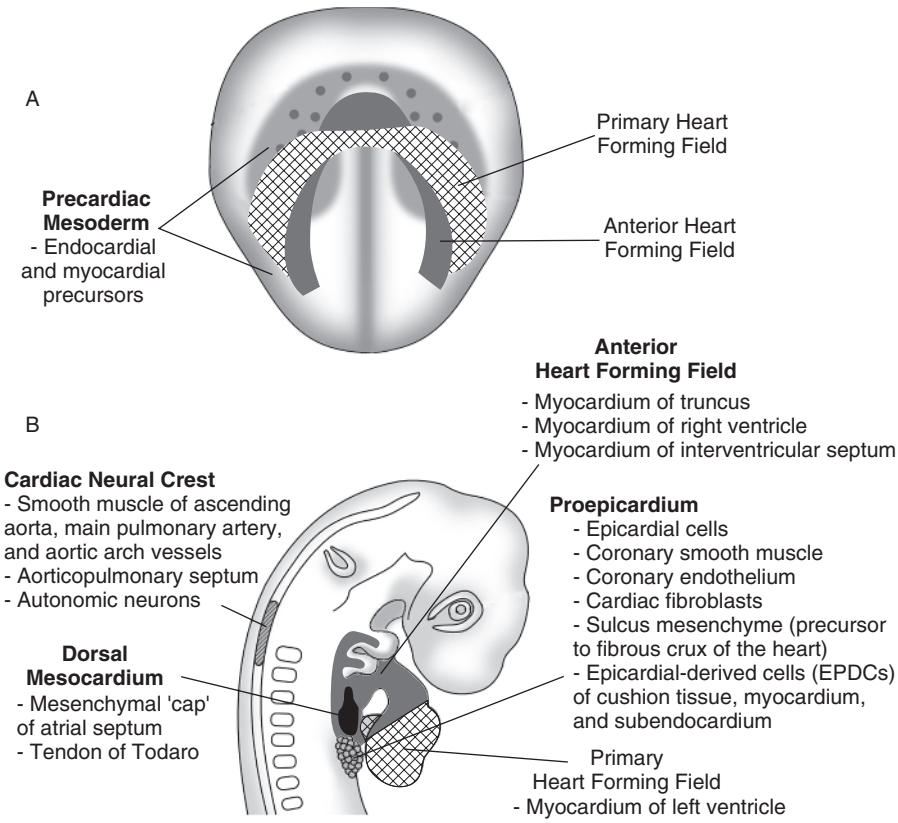

Figure 1.3 Normal heart development requires integration of cell populations from multiple sources. **A,** Precardiac mesoderm gives rise to the endocardium and the majority of cardiac cushion cells. Premyocardial cells give rise to the entire spectrum of cardiac myocyte phenotypes. The primary heart forming field will give rise to most of the myocardium of the atria and left ventricle. The anterior heart forming field will give rise to the myocardium of the outflow tract, right ventricle, and interventricular septum. **B,** Multiple extracardiac embryonic tissues provide critical cell populations to normal cardiac development. These cell populations include cardiac neural crest cells as well as cells from the proepicardium and the dorsal mesocardium.

heart field [25]. It is an important contributor to atrioventricular (AV) septation and serves as a conduit for the developing pulmonary veins. The dorsal mesocardium is also a pathway for cellular migrations as development proceeds, including neural crest-derived neural structures [27] and possibly cells derived from the ventral neural tube [28].

Soon after the formation of the cardiac tube the heartbeat is initiated and blood circulation can be observed (embryonic day 8.5 in the mouse and day 20 in the human). With the initiation of circulation the heart becomes the first organ to adopt its essential mature function in the embryo. At this point in cardiac organogenesis, however, the tube heart has not yet obtained its full complement of cell populations necessary for complete cardiac development. Early fate mapping studies [29–31] showed that the primary heart tube is derived from two bilateral fields of precardiac mesoderm, currently called the first heart field; this precardiac mesoderm was long considered the precursor tissue of the heart. Studies by others [32], however, strongly suggested that growth of the heart tube, specifically at the arterial pole, depended on the addition of cardiac tissue from a secondary pool of progenitor cells. It was not until the early twenty-first century that the nature of this additional cell population was elucidated. The combined studies of various laboratories [25,33–36] have provided significant new insights into the importance of this additional population of cells, called the second heart field, in the elongation and growth of the heart tube and in the formation of a mature four-chambered heart (Figure 1.3) [7]. Thus, these studies have demonstrated that the secondary heart field contributes at the arterial pole to the outflow tract and right ventricle and at the venous pole to parts of the atria and the dorsal mesenchymal protrusion.

The Tube Heart, Segments, and Segmental Identity

Traditionally, the heart tube has been regarded as containing the precursors of all of the cardiac segments. In reality, at the time the heartbeat is initiated the heart tube primarily consists of future left ventricular tissues [37,38]. Immunohistochemical, in situ hybridization, and cell fate tracing techniques have demonstrated that the outflow tract, the right ventricle [32], the AV junction segment [37], the atria [39], and the sinus venosus are added to the heart as looping proceeds. Indeed, these are the structures that are most important in the pathogenesis of the majority of forms of complex human congenital heart disease. Recent studies indicate that the outlet (truncal and conal) primordia [35,40] as well as the right ventricle and much of the

interventricular septum [35] and parts of the cardiac venous pole develop from the anterior/secondary heart field.

In prelooping and early looping stages the primitive heart tube consists of circumferential sheets of myocardial cells two to three layers thick surrounding an endothelial tube, these layers being separated by an acellular, extracellular matrix-rich space known as the cardiac jelly. As looping proceeds, the future segments can be distinguished morphologically by their position in the heart tube and by structural features, such as the striking accumulations of cardiac jelly in the AV canal and outflow segments. Segments can be distinguished physiologically by measurement of the differences in their velocity of muscular contraction and relaxation, their rates of spontaneous pacemaker activity, and the speed of electrical impulse conduction.

Segmental differentiation creates the physiological competence of the embryonic heart [41]. Unidirectional antegrade blood flow is maintained by organization of the tube heart into alternating regions of rapid and slow contractile properties [42]. The atrium has the fastest rate of spontaneous contractility and is the site of pacemaker activity. The wave of depolarization spreads from myocyte to myocyte from the atrium to the outflow tract, but the velocity of conduction is not uniform throughout the length of the heart tube. Atrial conduction is rapid, AV conduction is slow, ventricular conduction is rapid, and outlet conduction is slow. The zones of rapid conduction show rapid contraction–relaxation mechanical properties, while the slow zones of conduction demonstrate slow, sustained contractions. The result is a forceful contraction of the atria, followed by a sphincter-like contraction of the AV junction (prior to maturation of AV valves) that prevents the retrograde flow of blood during the forceful ventricular ejection phase. The cardiac cycle of the tube heart is completed by a sphincter-like contraction of the outflow tract (prior to maturation of the semilunar valves) to prevent retrograde blood flow from the aortic arches.

Genetic Determination of Cardiac Segmentation

In addition to functional differences, cardiac segments can also be distinguished by unique patterns of gene expression. However, despite the rapidly increasing number of markers that distinguish segments following heart tube formation, there has been less success in identifying segmental markers in the precardiac mesoderm. Data suggest that the final determination of lineage fate occurs in the precardiac mesoderm [9,31], but the timing and nature of the mechanisms are as yet poorly understood. Perhaps the best-studied determinants of the anterior–posterior axis in the gastrulating embryo are retinoids [43,44]. Retinoids are products of vitamin A metabolism, and manipulation of retinoid signaling pathways results in significant abnormalities in axial patterning in general and cardiac development in particular [45–49]. Abnormal development of atrial segments and systemic venous structures are observed in conditions of retinoid deficiency [50–52]. Excess retinoids create cardiac malformations, often involving the outflow tract [53,54], and result in ventricular expression of several genes that are normally largely restricted to the atria at these stages of normal development [55–57]. The spatial and temporal patterns of retinoid signaling in early cardiac development are highly correlated with the presence of retinaldehyde dehydrogenase 2 (RALDH2), a key enzyme in the retinol (vitamin A) to retinoic acid pathway [58–60]. Retinoid signaling pathways are clearly key mechanisms of segmental differentiation within the heart, but it is likely that other pathways yet to be determined are also involved.

Transgenic mice provide some of the most interesting data regarding differences between the genetic pathways regulating different regions of the heart. In these experiments, regulatory portions from one gene are used to drive the expression of a second gene whose product can readily be detected in the tissues. The DNA resulting from the combined portions of the two genes is injected into the male pronucleus of fertilized mouse eggs, and frequently the DNA is incorporated into the mouse nuclear DNA. The eggs are implanted in a female mouse and generally allowed to proceed through development until birth. The newborn animals bearing the new DNA (the "transgene") can be identified by analysis of their DNA. If the transgene is present, the animal will be bred and its offspring analyzed for the pattern of expression of the transgene.

Use of this technology has demonstrated several features of segmental and regional gene expression in the heart [61]. The genetic elements that determine regional patterns of gene expression are modular, in that genes expressed widely in the heart often have discrete portions of their regulatory DNA responsible for subsets of the overall pattern. For instance, a transgene driven by a 10-kilobase (kb) segment of the *Gata6* gene exhibits expression throughout the atria, AV junction, and left and right ventricles, excluding only the outflow tract; a smaller 2.3-kb fragment of the same gene drives expression only in the AV junction (Figure 1.4) [7,62]. The segmental and regional boundaries of gene expression determined by a specific genetic element may be variable during development, and transgenes expressed widely in the primitive tube heart can be restricted in their expression in the adult heart. Finally, the fact that some transgenes are differentially activated spatially and temporally in the heart is a striking confirmation of the nonequivalence of these tissues at the most basic level of gene regulation (Figure 1.4) [7].

Gene knockout experiments in mice also provide insight into the genetic regulatory networks critical to segmental differentiation. The requirement of the transcription factor HAND2 for normal development of the primitive right

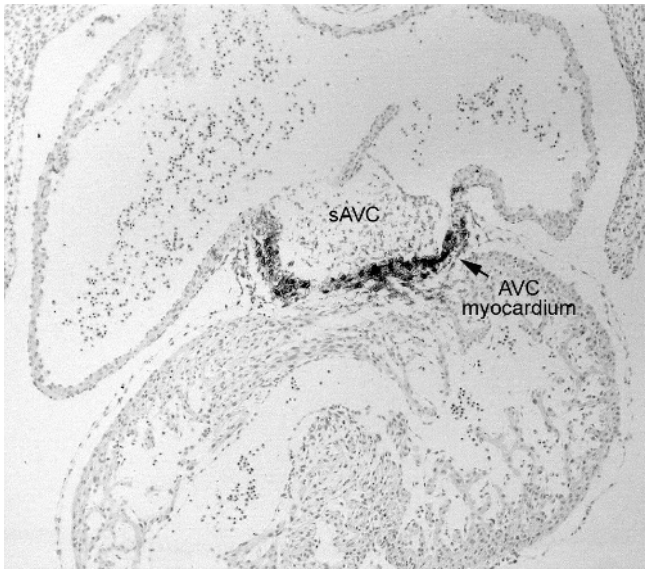

Figure 1.4 Section of an 11.75 embryonic day mouse embryo from a line carrying a transgene that expresses the LacZ reporter gene under the control of a portion of the GATA-6 promoter. At this stage of development expression of the LacZ gene, which produces the dark-staining cells indicated, is limited to atrioventricular canal myocardium. (sAVC, superior atrioventricular endocardial cushion; AVC, atrioventricular canal.) (Courtesy of A. Wessels and J. Burch.)

ventricle in mice is an especially compelling example of the apparent dependence of specific segments on specific genetic regulatory pathways [63].

A relatively new transgenic technique that has revolutionized the understanding of the developing heart is the use of Cre-lox mouse model systems [64]. In this approach mice are generated that contain the coding sequence for the Cre recombinase enzyme under the regulation of a gene sequence of interest. When these Cre mice are crossed with mice that carry sequences flanked by lox P sites, one can specifically delete these "Floxed" sequences and, depending on the nature of the Cre and Flox constructs, achieve, for instance, tissue-specific gene deletions [65] or cell fate tracing [25].

It is beyond the scope of this chapter to discuss in detail how each of the above techniques has advanced our insight into normal and abnormal cardiac development. For the interested reader there are some excellent recent reviews that discuss the use of these strategies [66,67].

Looping

As the heart tube extends due to addition of cardiac tissue to the arterial and venous poles, the heart tube bends to the right. As morphogenesis continues, the loop becomes more complex. The left ventricle moves inferior and anterior to the atrium, the right ventricle slightly anterior and to the right of the left ventricle. The bending of the heart tube is the first morphologic demonstration that the left and right sides of the embryo will not be morphologic mirror images, inextricably linking cardiac development to the correct establishment of the three body axes [68,69].

All vertebrate and most invertebrate body plans demonstrate fundamental asymmetries about the three body axes of anterior–posterior (A–P), dorsal–ventral (D–V), and left–right (L–R). At the molecular level, the axes are determined by asymmetric propagation of signaling events occurring very early in development. The process of L–R axis determination as it concerns heart development has been recently reviewed and broadly conceptualized as requiring three steps involving the initiation, elaboration, and interpretation of the sidedness signal [70,71]. The first step requires initiation of polarity along the A–P, D–V, and L–R axes. The initiating signals for these events are unknown in mammalian embryos. The second step is an elaboration and amplification of the initial L–R asymmetry through a variety of cellular signaling mechanisms. As is true in general for developmental processes, most of the molecules involved in elaborating the L–R signaling process in mice have easily recognized counterparts in birds. However, in a remarkable twist on that theme, some of the molecules required for left-sidedness in mice are determinants of right-sidedness in birds [72]. The molecules responsible for these processes in humans are poorly understood. The third step is the interpretation of the asymmetric signals elaborated in the second step by the cells and tissues of developing organs. The developmental fates of paired structures as to whether to form with mirror symmetries (such as the limbs), or as paired but unequal structures (such as the cardiac atria) is thus the result of both proper signal delivery to the organ primordia and proper reaction of the organ primordia to the signal.

As a measure of the complexity of the impact of genetic mechanisms on L–R axis determination on cardiac development, many genetic models of abnormal cardiac looping have now been described in mice [73]. Some are primarily models of abnormal directionality of looping, while others also show perturbation of the alignment of cardiac segments. Mouse models of globally randomized situs [74,75], situs inversus [76], situs defects affecting different embryonic organs to different degrees [77], and situs defects with preferential bilateral right- or left-sidedness have all been described [73]. Many of the genes implicated in the mouse models are candidate genes for heterotaxies in the human population [78].

The left and right atria have their molecular identities determined by L–R signaling mechanisms. Molecular distinctions between left and right atria are established early

after the atrial segment appears and are genetically dependent on L–R signaling mechanisms [79–81]. It is interesting to note, however, that there is often an increased incidence of transposition of the great arteries in mouse models of abnormal L–R axis determination [73], suggesting a possible element of L–R signaling in normal outflow development.

The mechanisms by which genetic signals result in regulated bending of the heart tube are unknown. Looping movements are intrinsic to the heart and will occur if the heart is isolated from the embryo, with or without beating [82,83]. The deformation of the straight heart tube into a looped structure likely results from some type of mechanical force [84]. However, the source of the required deforming force is not known. A simple explanation would be that myocytes replicate faster in the larger curvature of the loop and more slowly in the lesser curvature, and data suggesting a contribution of regional differences in growth have been presented [85,86]. However, cytochalasin B, an inhibitor of actin polymerization and therefore an inhibitor of cytoskeletal rearrangements, is also capable of either abolishing looping or reversing the direction of looping, according to whether it has been universally applied or selectively applied [87]. This suggests that the required asymmetric mechanical tension may be generated within the cells of the tube heart in response to as yet unknown regulatory signals.

Looping, Convergence, and Septation – Key Landmarks

Looping determines not only the sidedness of the heart but also the correct relationship of the segments of the heart to each other. Imaginary but useful divisions can be assigned to the morphogenetic steps leading from the more-or-less straight heart tube to the looped but still tubular heart, and from the looped heart to the heart poised for septation. Therefore, in this chapter, looping describes the initial period of growth, bending, and twisting of the heart tube. Looping begins and ends with the AV junction connected solely to the left ventricle and the outflow tract connected only to the right ventricle. The second phase of looping, sometimes called convergence, is the process of bringing the right atrial inflow over the right ventricle and the aortic outflow tract over the left ventricle, in the process aligning the outflow septal ridges for fusion with the primitive muscular septum and AV cushions. Ventricular septation is the process of closing the primary interventricular foramen while bringing the interventricular septum into continuity with the conus septum. Descriptions of these processes require recognition of a relatively small number of critical landmarks present in the embryonic heart during the looping and convergence stages of development (Figure 1.5) [7,88].

The looped heart has an inner curvature and an outer curvature. By nature of the tight angulation of the inner curvature the primitive atrial, AV, ventricular, and outflow segments are in close proximity for the remainder of cardiac development. As the region where the right ventricle acquires its inflow and the left ventricle acquires its outflow, the inner curvature of the heart is arguably the most critical, complex, and dynamic site in normal cardiac development.

On the lumenal surface of the heart, the fold in the heart at the inner curvature results in a small muscular ridge inside the heart between the AV junction and the outflow tract called the ventriculoinfundibular flange or ridge. Other key landmarks are the two major endocardial cushions of the AV junction and the two endocardial ridges of the outflow tract. The inferior endocardial cushion is attached to the dorsal AV myocardium and the superior endocardial cushion is attached to the ventral atrioventricular myocardium. As convergence proceeds, small right and left lateral AV endocardial cushions will become visible. The two outflow tract endocardial cushions form extended spiral ridges from the end of the truncus distally to the body of the right ventricle caudally. The endocardial cushion ridge ending in the anterior right ventricle is called the septal endocardial ridge. The endocardial ridge terminating posteriorly in the right ventricle is called the parietal endocardial ridge. The parietal endocardial ridge makes contact with the right lateral endocardial cushion, which itself will become continuous with the superior endocardial cushion. The septal endocardial ridge will make contact with the inferior endocardial cushion. As the endocardial cushions fuse during normal septation, they create, together with the mesenchymal cap of the primary atrial septum and the dorsal mesenchyme protrusion, the central AV mesenchymal complex extending from the AV junction to the distal extent of the myocardial outflow tract. At the most basic level the process of fusion of mesenchymal tissues can be thought of as a tissue zipper that septates the heart [26]. The reason that the endocardial cushion tissues of the conus septum cannot be found on inspection of the mature heart is that these mesenchymal structures are replaced by myocardium in the process known as myocardialization [89]. With respect to human congenital heart disease, this is a critical series of events, as disease phenotypes such as complex transposition, truncus arteriosus, and a number of tetralogy phenotypes all derive from aberrations of these normal developmental steps.

The left and right ventricular lumens are in continuity through the primary interventricular foramen. From the right ventricle, blood passes into the outflow tract of the heart. A myocardial cuff extends along the outflow tract to the junction with the aortic sac at the level of the pericardial reflection.

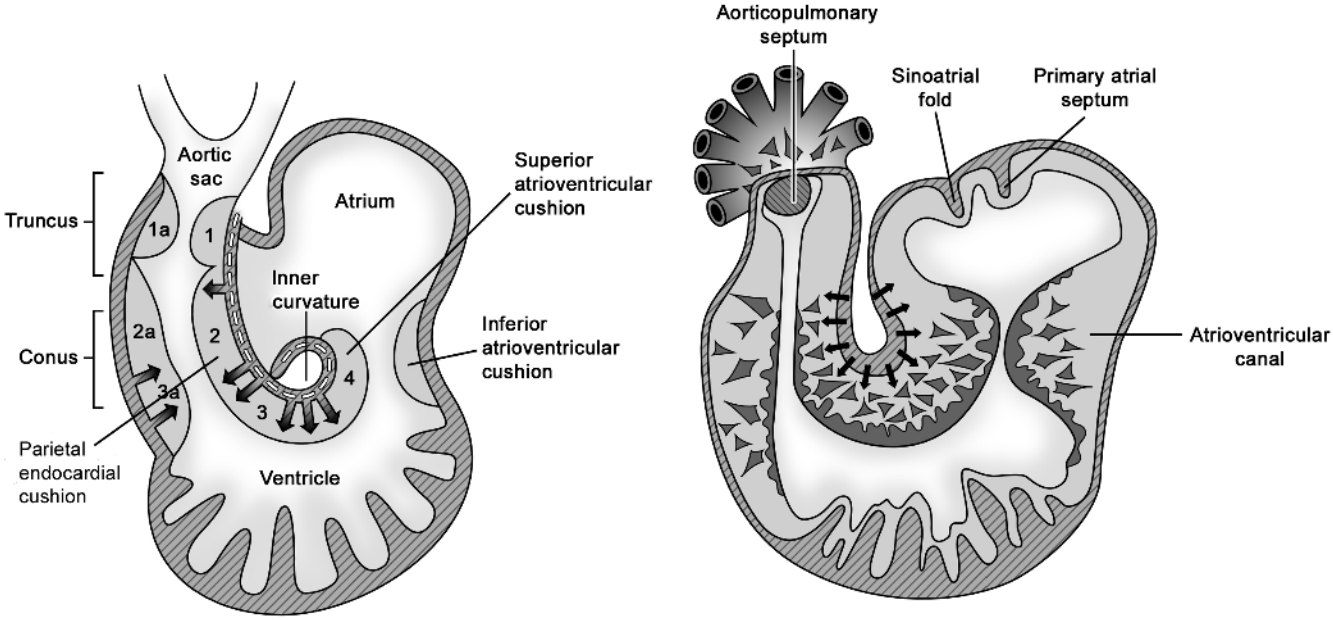

Figure 1.5 Highly simplified representation of key cardiac landmarks in early cardiac development. On the left, the cartoon illustrates the relative positions of the endocardial cushions at approximately HH stage 24. The truncal cushions are indicated as 1 and 1a, the distal conal cushions by 2 and 2a, the proximal conal cushions by 3 and 3a, and the superior atrioventricular cushion by 4. The arrows indicate the future sites of myocardialization. At the inner curvature, normal development results in loss of the myocardial sleeve and retention of the primitive fibrous continuity between the parietal endocardial cushion and the superior atrioventricular cushion. This is reflected by the fibrous continuity of the mitral valve and the aortic valve observed in the normal mature heart. In the cartoon on the right, the myocardialization of the inner curvature is indicated by the arrows; the mesenchymal invasion of the endocardial cushions is indicated by the polygonal cells. (After Mjaatvedt CH, Yamamura H, Wessels A, Ramsdell A, Turner D, *et al.* (1999) Mechanisms of segmentation, septation, and remodeling of the tubular heart: endocardial cushion fate and cardiac looping. In: Harvey RP, Rosenthal N, editors. *Heart Development*. San Diego: Academic Press. pp. 159–175 [88].)

During convergence, the angle of the inner curvature of the heart becomes more acute. The right AV junction is formed by rightward expansion of the AV junction, while at the same time the major (or midline) AV endocardial cushions are approaching each other in the center of the lumen of the AV junction. The outflow endocardial ridges, although unfused, define distinct aortic and pulmonary channels. The aortic channel moves leftward and anterior of its original position. Because of the combined rightward expansion of the AV orifice and the leftward movement of the aortic outflow tract the acute angle of the inner curvature now defines the region where the AV junction and the outflow tract are in continuity. These same morphogenetic movements result in rotation of the outflow ridges to a plane that is closer to parallel to that of the growing muscular septum.

Endocardial Cushion Development and Myocardialization

When the tube heart initially forms, the myocardial and endocardial cell layers are separated by an acellular substance traditionally called "cardiac jelly" [90]. Cardiac jelly can be regarded as a basement membrane, as it lies between two juxtaposed epithelia (the myocardium and the endocardium) and contains traditional basement membrane proteins. The initial production and distribution of these molecules is largely controlled by factors produced by the associated AV myocardium [91,92]. Cardiac jelly condenses into opposing swellings at the outflow and AV regions of the early, looped heart. The resulting endocardial cushions function in combination with the specialized contractile properties of the AV junction and outflow tract myocardium to prevent reversal of blood flow [93]. The AV endocardial cushions also function as the substrate for the formation of the mesenchymal tissues of the crux of the heart, including the AV valves and central fibrous body [94]. Endocardial cushions of the embryonic outflow tract participate in the formation of the aorticopulmonary septum, semilunar valves, and conus septum [95]. During morphogenesis of the endocardial cushions, the mesenchymal cell population that populates the originally acellular cardiac jelly is derived from the endothelial cells of the heart [67,96] along with a population of epicardially

derived cells that also migrates into the AV cushions, but not the outflow tract cushions [97].

Endothelial invasion of the cardiac jelly results in a true transdifferentiation of cell phenotype, from a cell within a typical epithelium to an independently migratory, fibroblast-like mesenchymal cell [98–100]. This process has been compared to cellular changes during malignant transformation and is at least partially under the control of TGFβ-mediated signaling processes [101,102]. Only endocardium from the outflow tract and AV cushions are competent to undergo transformation, and only outflow tract and AV junction myocardium are able to induce transformation [101,103]. Not all the endocardial cells of the AV and conotruncal regions participate in these changes; as migration proceeds, residual endocardial cell populations undergo divisions to replenish their numbers. The mesenchymal cells also replicate actively to populate the cushions [99]. Recent data suggest that a similar process may result in an endothelial-to-mesenchymal transformation contributing to the neointima of atheromatous plaques [104].

Myocardialization is the process in which the mesenchyme of the endocardial cushions is replaced by myocardium [89]. All of the septal structures inside the heart – the interventricular septum, the atrial septum, and the conal septum – are created in part by fusion of nonmyocardial mesenchymal cushions. Myocardialization is responsible for the formation of the myocardial conus septum and the inlet and anterior outlet portions of the interventricular septum. In humans, the AV membranous septum is the only nonmyocardial septal structure derived from endocardial cushion tissue. The myocardialization of the conal cushions appears, based on Cre-lox cell fate studies, to primarily involve myocardial cell invasion of the cushion tissue. The mechanisms controlling this process are unclear [89,105,106].

Atrial Septation

Atrial septation and connection of the common pulmonary vein to the left atrium are closely related events in the normal heart [81]. Recent investigations in mouse, chick, and human embryos highlight the importance of the dorsal mesocardium to these events. At the site where the dorsal mesocardium is in continuity with the atrium (approximately the level of the lung buds) there is a protrusion of mesenchymal tissue into the atrium. This tissue has been recognized for many years and by a variety of names, including "spina vestibuli," "endocardial proliferation of the dorsal mesocardium," "sinus venosus tissue," and, most recently, the "dorsal mesenchymal protrusion" – the terminology adopted herein. Unlike other mesenchymal tissues in the AV junction, the dorsal mesenchymal protrusion is not derived from an epithelial-to-mesenchymal transformation, but rather is a derivative of the second heart field [25,26]. The dorsal mesenchymal protrusion extends into the atrial cavity and is contiguous with the mesenchymal cap on the leading edge of the septum primum. Together with the two major atrioventricular cushions, the dorsal mesenchymal protrusion and the cap eventually fuse to form the atrioventricular mesenchymal complex. This process is essential for normal atrioventricular septation (Figure 1.6) [7,81]. Recent papers strongly suggest that perturbation of the development of the dorsal mesenchymal protrusion might be one of the major mechanisms in the pathogenesis of atrioventricular septal defects.

Based on the expression of several molecular markers that distinguish between left and right atrial myocardium [81], the myocardial portion of the septum primum is derived from left atrial myocardium. Growth of the septum primum occurs by lengthening of its myocardial portion. As described above, the mesenchymal cap on the leading edge of the septum primum is mesenchymal, the cells being derived by endothelial-to-mesenchymal transformation similar to that seen in the endocardial cushions [67]. As growth of the septum primum proceeds, it brings the mesenchymal cap of the septum, as well as the dorsal mesenchymal protrusion into contact with the two major AV endocardial cushions (Figure 1.7) [25,26]. The primary interatrial foramen is closed by fusion of these mesenchymal tissues as they form the AV mesenchymal complex [26]. Knowledge of this process is critical towards understanding the pathogenesis of complete common AV canal, as well as understanding the tissue relationships relevant to its repair.

Before the closure of the primary interatrial foramen occurs, the foramen secundum appears in the body of the septum primum. In humans, this process is initiated by the appearance of small fenestrations that increase in number and size until they coalesce into a definitive foramen secundum [81].

The septum secundum forms as an infolding of the atrial roof in the intervalvar space between the left venous valve of the sinus venosus and the septum primum. The septum secundum also marks the site of boundary between left atrial and right atrial tissues. As a result, the left atrial myocardium of the septum secundum exhibits left atrial markers while the right atrial myocardial surface of the septum secundum exhibits right atrial markers [81].

Interventricular Septation

As the primary interventricular foramen initially provides all of the inflow to the right ventricle and the entire outflow for the left ventricle, its correct closure is critical to normal cardiac development. Closure of the primary interventricular foramen is accomplished through coordinated growth of the muscular interventricular septum and fusion of

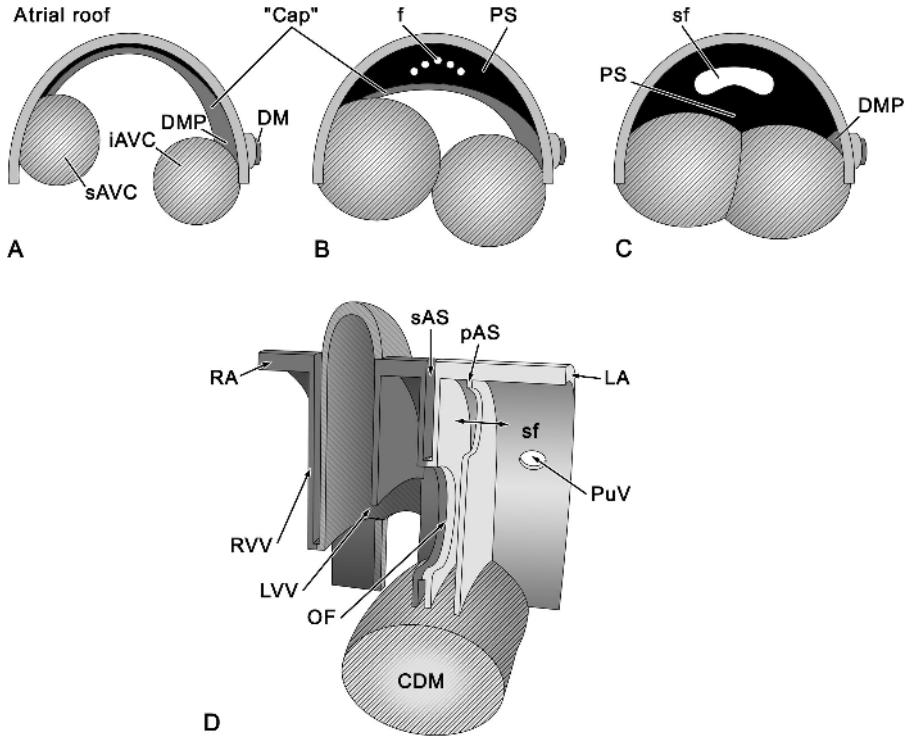

Figure 1.6 Sequence of events in atrial septation in human development. **A,** Heart at approximately 4.5 weeks of development. The leading edge of the septum primum is covered by a mesenchymal cap that is in continuity with the protrusion of the dorsal mesocardium into the atrial cavity. The superior and inferior atrioventricular cushions (sAVC and iAVC) are also in continuity with the mesenchymal cap. (DM, dorsal mesocardium; DMP, dorsal mesocardial protrusion.) **B,** Heart at ~6 weeks development. The septum primum with its mesenchymal cap is approaching the fusing inferior atrioventricular cushion and superior atrioventricular cushion. Fenestrations (f) are appearing in the muscular septum primum (PS). **C,** At ~6–7 weeks of development the fusion of the sAVC, iAVC, and cap of the septum primum is complete. The multiple fenestrations in the septum primum coalesce, forming the secondary foramen (sf). **D,** The secondary atrial septum (sAS) is created by infolding of myocardium at the junction of left and right atrial myocardium. Use of molecular markers distinguishing different populations of sinoatrial myocardial cells shows that the right-sided fold of the sAS and left venous valve (LVV) are derived from right atrial (RA) myocardium, while the left-sided fold of the sAS and primary atrial septum (pAS) are derived from left atrial (LA) myocardium. The right venous valve (RVV) is formed by infolding at the site of juncture of sinus venosus (SV) myocardium and RA myocardium, resulting in an RA molecular phenotype on the atrial surface and a SV molecular phenotype on the luminal surface. (CDM, endocardial cushion-derived mesenchyme; PuV, common pulmonary vein; OF, foramen ovale.) (After Wessels A, Anderson RH, Markwald RR, *et al.* (2000) Atrial development in the human heart: an immunohistochemical study with emphasis on the role of mesenchymal tissues. Anat Rec 259, 288–300 [81].)

endocardial cushions in the AV junction and the outflow tract.

Growth of the muscular interventricular septum is closely associated with dynamic changes in patterning of the ventricular myocardium [107]. When the heart tube initially forms and early after looping, its myocardial layers are but a few cells thick. After looping, the ventricular chambers enlarge caudally in a pouch-like fashion. The pouches are located on the greater curvature of the looped heart and quickly develop a series of circumferential ridges on their internal surfaces (Figure 1.8) [7,107].

The myocytes of the primitive trabecular ridges differ from the subjacent compact myocardium in that the myocytes of the compact myocardium are actively proliferating, while the trabecular myocytes have withdrawn from the cell cycle and are not dividing [107]. The "germinal layer" of compact myocardium provides increases in the numbers of ventricular wall myocytes, but the initial major increases in myocardial mass occur through increase in the trabecular component of the myocardium [107]. The compact myocardium "feeds" cells into the ventricular junctions of the developing trabeculae; this is a relationship that persists throughout embryonic myocardial growth [107].

The primitive trabecular ridges become fenestrated and sheet-like as they expand. Trabeculae are believed to

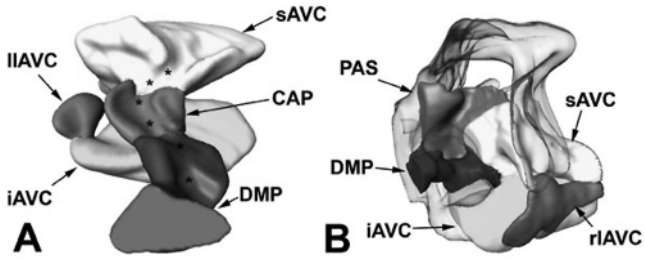

Figure 1.7 Three-dimensional reconstructions demonstrating the spatiotemporal relationships of the atrioventricular mesenchymal tissues during mouse heart development. Computer-generated three-dimensional reconstructions (AMIRA software) based on stained serial sections of mouse hearts **A** at embryonic day 11.5 and **B** at embryonic day 13. These panels show how the respective bodies of mesenchyme fuse with each other to accomplish atrioventricular septation. **A,** The mesenchymal tissues are viewed from above, while all other cardiac tissues are digitally removed to facilitate the study of the relationship of the mesenchymal components. At this stage, the individual mesenchymal components have not fused completely yet. The asterisks mark the groove within these tissues where the myocardial part of the septum primum is located (removed for reconstruction). **B,** The AV tissues are viewed as if one was standing in the right atrium. At this stage, all the mesenchymal tissues have fused. This panel demonstrates how the dorsal mesenchymal protrusion forms a wedge between the major AV cushions at the same time forming the base of the septum primum. At this stage the atrial cap cannot be distinguished any longer from the other endocardially derived mesenchymal tissues (for more detailed description see Snarr *et al.* [25,26]. (CAP, mesenchymal cap on the primary atrial septum; DMP, the dorsal mesenchymal protrusion; iAVC, inferior AV cushion; llAVC, left lateral AV cushion; PAS, primary atrial septum [septum primum]; rlAVC, right lateral AV cushion; sAVC, superior AV cushion.) (Reproduced with permission from Snarr *et al.* [26].)

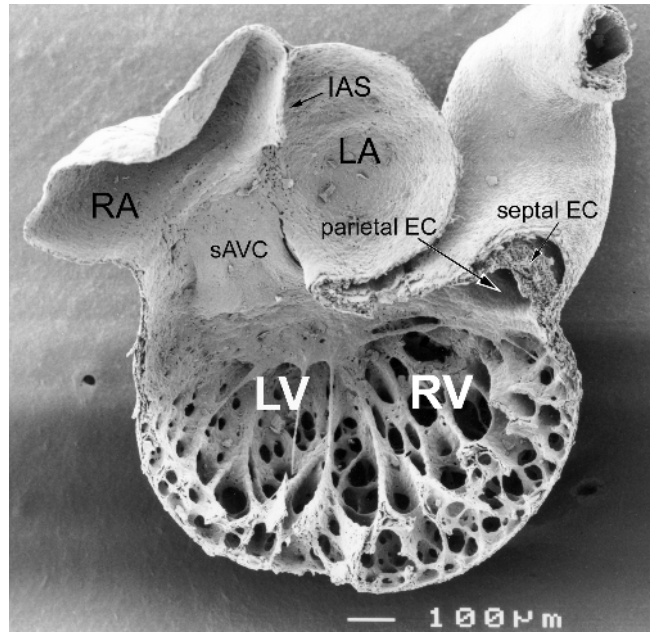

Figure 1.8 Scanning electron micrograph of a section through the right and left ventricles of an embryonic chick heart. The pleat-like ridges characteristic of early myocardial trabeculum formation are easily appreciated. At this stage, the inner curvature of the heart separates the atrioventricular inflow from the right ventricle and the outflow tract from the left ventricle. (EC, endocardial cushion; IAS, interatrial septum; LA, left atrium; RA, right atrium; sAVC, superior atrioventricular cushion.) (Courtesy of David Sedmera.)

assume several physiologic functions in the primitive heart. They enhance contractile function of the ventricles [108]. The surface area of the endocardium is greatly increased by the presence of trabeculae, which is believed to improve nutrient and gas exchange with the developing myocardium before the development of a true coronary vasculature [109]. The trabeculae have been asserted to be the conduction system equivalent to (and possibly precursors to) the distal bundle branches and Purkinje fibers in the developing heart [42]. Trabeculae also help to direct the flow of blood in the preseptated heart [110]. Thus, the infrequent, yet important echocardiographic finding of ventricular noncompaction bears important implications.

In the chick heart, the primitive muscular septum is initially formed by a coalescence of trabeculae. In the mammalian heart, the primitive muscular septum appears to be the product of infolding of the compact myocardium produced by growth of the ventricular apices. Perhaps as a consequence, the interventricular groove is a more distinctive feature of mammalian hearts than avian hearts. The leading edge of the primitive muscular septum in humans is readily identified by the HNK1-Leu7 antibody that characterizes the primary ring (Figure 1.9) [7,111,112]. Use of this antibody in human embryos clearly demonstrates that the myocardial precursors of the right ventricle and right ventricular septum, including the inflow segment, are derived in their entirety from myocardial cell populations distal to the original primary interventricular foramen [113].

The primitive muscular interventricular septum is initially a crescent-shaped structure that extends at its posterior limit to the inferior endocardial cushion and at its anterior limit to the superior endocardial cushion. Part of the process of closure of the primary interventricular foramen consists of expansion of the superior and inferior endocardial cushions towards each other, where they will make contact and fuse at approximately 6 weeks' gestation in the human. The mechanism of fusion of the endocardial cushions in spite of the continuous mechanical activity of the heart is not known, but certainly deserves respect.

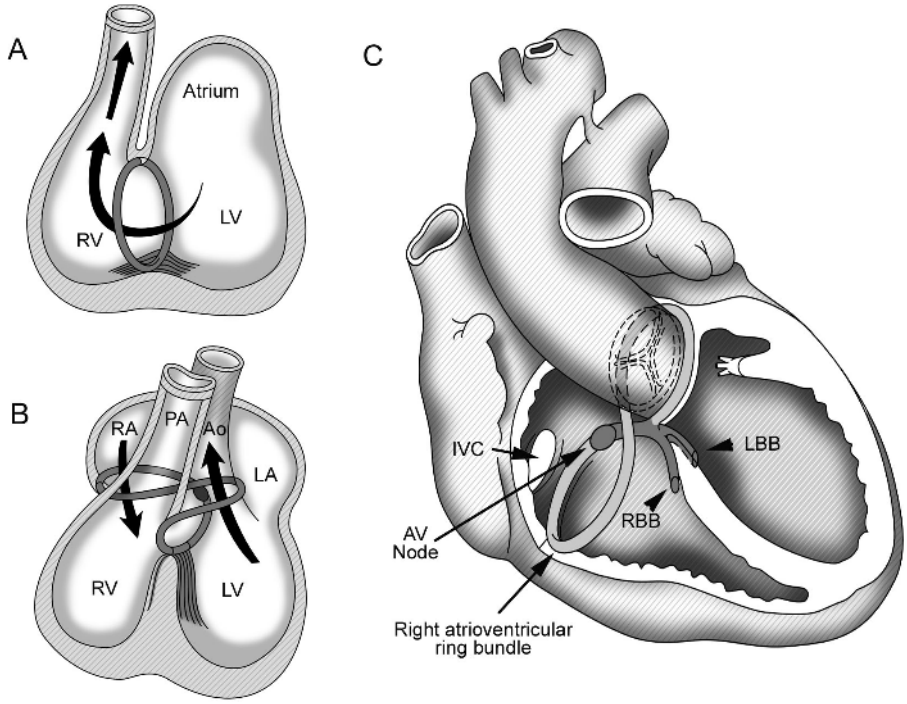

Figure 1.9 These diagrams demonstrate the development of the conduction system from a ring of myocardium detected in human embryonic heart by their expression of a carbohydrate epitope recognized by the antibodies Gln2, HNK1, and Leu7. **A,** Human heart at roughly 5 weeks' gestation. A ring of myocardium surrounding the primary interventricular foramen is detected. Note that the superior aspect of the ring is at the junction of atrioventricular (AV) myocardium and ventricular myocardium. **B,** In the human heart of roughly 7 weeks' development, convergence has resulted in expansion of the small segment of AV junctional myocardium to the right, accompanying the rightward expansion of the AV inlet. The leftward movement of the outlet results in the looping of the ring around the aortic root. As the muscular ventricular septum begins to grow, strands of ring tissue can be found extending from the major aspect of the ring on the crest of the septum down the septal walls towards the expanding apices of the right and left ventricles. **C,** The mature cardiac conduction system of AV node, bundle of His, and right bundle branch (RBB) and left bundle branch (LBB) is derived from the primitive ring tissue. In addition, remnants of the primitive ring in the adult heart can be found on the atrial side of the tricuspid valve fibrous annulus as well as in retroaortic myocardium. (RV; right ventricle, LV, left ventricle; RA, right atrium; LA, left atrium; PA, pulmonary artery; Ao, aorta; IVC, inferior vena cava.) (After Wessels A, Vermeulen JL, Verbeek FJ, *et al.* (1992) Spatial distribution of "tissue-specific" antigens in the developing human heart and skeletal muscle. III. An immunohistochemical analysis of the distribution of the neural tissue antigen G1N2 in the embryonic heart; implications for the development of the atrioventricular conduction system. Anat Rec 232, 97–111 [111]; and Moorman AFM, Lamers WH (1999) Development of the conduction system of the vertebrate heart. In: Harvey RP, Rosenthal N, editors. *Heart Development*. San Diego: Academic Press. pp. 195–207 [112].)

Further growth of the interventricular muscular septum results in fusion of the crest of the septum with the fused cushion. The boundaries between the original muscular septum and endocardial cushion-derived portions of the septum become obscured by myocardialization except for the membranous septum between the left ventricle and right atrium. Normal inlet septum development is primarily determined by interactions between the inferior endocardial cushion-derived tissue and the muscular ventricular septum, while the smooth anterior interventricular septum is derived from interactions between the superior endocardial cushion and the muscular septum. The membranous septum is the approximate site of final union between the muscular septum and the superior and inferior endocardial cushions [114].

The Atrioventricular Junction Segment and Atrioventricular Valve Development

The electrophysiologic and physiologic properties of the junctional myocardium between the primitive atria and ventricles are critical to the preseptated heart, as previously discussed. However, myocardial continuity between the AV junctional myocardium, the atrial myocardium, and the ventricular myocardium must be interrupted for the development of the fibrous crux of the heart and the correct

function of the conduction system. This is accomplished by formation of a layer of fibrous insulation called the annulus fibrosis that will completely interrupt myocardial continuity between the AV myocardium and the ventricular myocardium, with the exception of the penetrating bundle of His specialized myocardium. In the mature heart the remnants of AV junction myocardium become incorporated into the myocardium of the definitive atrium [94].

Fibrous interruption of AV myocardial continuity results from the fusion of mesenchymal cell populations of the AV endocardial cushions with a mesenchymal cell population found in the atrioventricular sulcus on the external surface of the looped heart. Atrioventricular sulcus mesenchyme cells are brought to the heart in the course of the epicardial cell migration (see Figure 1.3) [7], as discussed in greater detail later in this chapter in connection with coronary artery development. Morphologic studies suggest that the sulcus mesenchyme actively invaginates into the endocardial cushions [115]; the mechanisms driving mesenchymal invagination and the parting of the myocardial layer are unknown. Interruption of myocardial continuity begins at 52 to 60 days of gestation in the human heart and is normally "complete" by the fourth month of gestation [94]. Failure to form the insulating tissues of the AV junction may underlie clinical pre-excitation syndromes. Interestingly, isolated myocytes possibly representing remnants of the embryonic junctional myocardium, originally present between the sulcus mesenchyme and the endocardial cushion mesenchyme, have been identified bridging the fibrous insulation of normal neonatal hearts [116]. This location is different from that noted for parietal accessory atrioventricular bundles [117], which are described as subepicardial and, therefore, seem to represent a different myocardial path through the sulcus mesenchyme-derived fibrous tissue. No structures similar to parietal accessory AV connections are noted in the course of normal development. Thus, the possibility that these accessory connections develop postnatally should be considered. The relationship between pre-excitation pathways in general and normal morphologic events requires further investigation.

Atrioventricular valve development may be tied to the process of sulcus tissue ingrowth, as the hinge points of the definitive leaflets are normally found at the point of juncture between the endocardial cushion tissues and the invaginating sulcus tissue. Atrioventricular valve leaflets are formed by separation of endocardial cushion tissue and myocardium from the ventricular walls in the poorly understood process of delamination [105,118,119]. Other events occurring at the same time that certainly influence normal valvar morphogenesis and may contribute to the delamination process include coarsening of the ventricular trabeculae, incorporation of trabeculae into the compact myocardium, and apical expansion of the ventricular cavity.

At the time of delamination, the atrial surfaces of the valve leaflets are composed of endocardial cushion tissue while the ventricular surfaces are primarily myocardial. The myocardial layer provides continuity with the evolving subvalvar tension apparatus. As leaflet morphogenesis proceeds, the myocardial component is eliminated by unknown processes. Initially, the ends of the AV leaflets are connected to the compact ventricular myocardium either directly or via trabecular outgrowths of the myocardium. As development proceeds, papillary muscles are derived by two mechanisms: from initially independent, preexisting trabeculae coalescing together to form papillary muscles; and from delamination of myocardium into myocardial structures that join with trabeculae or form of themselves the papillary muscles. The mitral valve papillary muscles are derived from a single large trabecula that then separates into the two independent papillary supports [119]. Thus the surgically challenging group of patients with parachute mitral valve derivatives are likely due to deficiencies in this process. Tricuspid valve papillary muscles develop independently from each other and via different mechanisms; the anterior papillary muscle of the tricuspid derives from an early coalescence of trabeculae detectable at 6 weeks' gestation, the septal leaflet papillary muscle is a product of delamination during the tenth to twelfth week of gestation, and the posterior papillary muscle complex is still a relatively indistinct structure at 12 weeks' gestation [105]. Chordae are formed by progressive fenestration and fibrous differentiation of trabeculae and/or the initially solid individual valve leaflets; there is disagreement with respect to the derivation of chordae from myocardium or endocardial cushion tissue [105,107,118].

As previously noted, there are four endocardial cushions in the AV junction. The superior and inferior cushions are the most prominent endocardial cushion masses from their first appearance, but there are also important contributions from the lateral endocardial cushions, which are visible only after Carnegie Stage 17 (approximately 42 days) [94,118]. The left lateral cushion contributes to the posterior (mural) leaflet of the mitral valve. The right lateral cushion, which becomes continuous anteriorly with the septal endocardial cushion of the outflow tract, contributes to the formation of the anterior and inferior leaflets of the tricuspid valve.

Atrioventricular valve morphogenesis is one of the most prolonged aspects of human cardiac development. Recognizable elements of the tricuspid valve begin formation at 5–6 weeks' gestation. The AV endocardial cushions are actively reconfiguring at this time, with fusion of the superior and right lateral AV endocardial cushions to each other. The conal cushions are also completing their fusion during this time. The fused outflow septum then expands apically to reach the inner curvature of the heart, anterior to the fusing superior and right lateral endocardial

cushions. In this position the fused outflow cushions will become adherent to the myocardium of the ventriculoinfundibular fold, establishing the anterior position of the conus septum with respect to the atrioventricular valvular structures, and also forming the crista supraventricularis [105]. Despite the overall advanced stage of cardiac morphogenesis at this point, the tricuspid valve leaflets are still very primitive in appearance and not freely mobile. The inferior leaflet is fully delaminated by the end of the eighth week of gestation, the anterior leaflet by the eleventh week, and the septal leaflet in the twelfth week. The commissure separating the anterior and septal leaflets is not complete until the septal leaflet is fully delaminated [105].

In development of the mitral valve, the inferior and superior AV cushions begin to fuse at roughly 5 weeks' gestation; even before fusion, the enlarged trabecular complex that will evolve into the two mitral papillary muscles can be seen connecting the superior and inferior cushions [118,119]. The left lateral cushion, the precursor to the posterior leaflet, is visible by the seventh week of gestation. At approximately this time initial delamination of the mitral valve structures becomes detectable and continues until the tenth week of development. Between the tenth and fourteenth weeks of development myocardial elements of the leaflets are eliminated, papillary muscles achieve their adult appearance, and chordae differentiate [118,119].

Development of the Conduction System

The sinoatrial node first becomes detectable at approximately 10.5 days in mouse development, roughly equivalent to Carnegie stage 14 (approximately 32 days) of human development, at the medial wall of the right common cardinal vein and extending cranially to the junction of the anterior and common cardinal veins. This corresponds to what will become the portion of the superior vena cava between the orifice of the azygous vein and the right atrium in the adult [120].

In the human embryo the AV node becomes detectable histologically at approximately Carnegie stage 15 (approximately 33 days) [121]. It is located in the posterior portion of the AV canal in the myocardium under the ventricular margin of the inferior endocardial cushion and is included in the primary ring [94]. The primitive AV node is in direct continuity with the AV and ventricular myocardium. From the earliest stages a cellular tract destined to become the bundle of His can be noted extending from the main mass of AV nodal tissue to the ventricular subendocardium. The AV sulcus mesenchyme will invaginate to make contact with the endocardial cushion mesenchyme inferiorly to the main mass of the developing AV node while encasing the future bundle of His in the fibrous insulating tissue at the crux of the heart [94].

The proximal bundle branches are detected in the human by antibodies to the primary ring antigen Gln2/HNK1/Leu7 (Figure 1.9) [7,111,112]. Differentiation of conduction tissue in the ventricles appears to occur by a process of recruitment of "working" myocardium into the conduction lineage and to be associated with withdrawal from the cell cycle [122,123]. Numerous observations support the contention that the trabeculae of the primitive heart are the initial conduction pathways connecting the proximal bundle branches with the ventricular free walls [124]. Subsets of trabeculae probably remain as elements of the conduction tissue in the mature heart.

The cellular morphology of Purkinje fibers is extremely variable between species [125]. In some species intramural Purkinje fibers are very difficult to distinguish by morphologic criteria. Molecular markers that unambiguously identify intramural Purkinje fibers across species are not known [124]. However, in all animals in which they have been studied, intramural Purkinje fibers are late-appearing structures in comparison to the central AV node–His bundle–bundle branch conduction tissues. In the developing sheep heart, where Purkinje fibers are easily distinguished by morphologic criteria from "working" ventricular myocytes, intramural Purkinje fibers are not seen until 60 days' gestation, while the AV node becomes visible as early as 27 days' gestation [126]. In this species, morphologic differentiation of the conduction tissue clearly progresses outward from the AV node.

Purkinje fibers in the chick embryo myocardium can be recognized by specific expression of the gap junction protein Cx42. Use of this marker shows that chick embryo Purkinje fibers are only detectable at day 10 of chicken development. In this model ventricular myocytes are recruited to differentiate into Purkinje cells only in the vicinity of developing coronary arteries [123]. Data suggest that endothelin signaling may be an important determinant of this process [127].

Morphogenesis of the Outflow Tract

Landmarks in the Outflow Tract

The morphologic terminology for the outflow tract used in this chapter follows that proposed by Pexieder [128]. The outflow tract is relatively short in the early phases of looping, after which it becomes elongated, with a distinct bend. The site of the bend is the primary external landmark dividing the truncus from the conus portions of the outflow tract: separate structures. The external landmarks for the entire region are the ventriculoinfundibular fold proximally and the aortic sac distally. The aortic sac–outflow junction is identified by flaring of the root of the aortic sac, the reflection of the pericardium, and the distal limit of the cardiac jelly and myocardium. The proximal end of the

outflow tract lumen is marked by myocardial ridge on the inner surface of the ventriculoinfundibular fold, the ventriculoinfundibular flange. The septal outflow ridge and parietal outflow ridge spiral from the right ventricle to the distal outflow tract, with a distinct change in their direction noted at the site of the bend in the outflow tract. As septation proceeds, the myocardial outflow tract shortens.

At the base of the heart the conal ridges are continuous with the AV endocardial cushions. During remodeling of the conus the mesenchymal (fibrous) continuity of the cushions will be retained between the mitral and aortic valves but will be lost between the tricuspid and pulmonary valves. The mechanisms through which outflow tract remodeling occurs are of great interest but remain largely undetermined. It is precisely these mechanisms that are of particular importance in understanding the pathogenesis of a large number of clinically challenging congenital heart disease phenotypes. Indeed, the normal processes of outflow tract remodeling are easily disrupted via pharmacologic, genetic, or experimental microsurgical manipulations, often resulting in persistence of a complete myocardial conus for both semilunar valves and a ventricular septal defect – double-outlet right ventricle (DORV) [129,130]. In one experimental model in which a clip was placed on a vitelline vein, the resulting malformation appeared to be secondary to altered embryonic blood flow; however, this model of altered blood flow does not explain the vast majority of congenital heart disease phenotypes [129,131,132]. Indeed, different teratogenic models are capable of resulting in different forms of conal abnormalities within the spectrum of DORV [129]. The frequency with which DORV is observed in experimental models presumably points to the requirement for integration of multiple processes for the embryonic heart to proceed beyond the "default" relationship of having both great arteries arising from the right ventricle. It also points out that the terminology "DORV" may undesirably lump an etiologically disparate group of defects into one final common pathway lesion. Thus, careful analysis of vessel morphology is required to accurately determine the cardiac phenotype. Alternatively, varieties of DORV may be forms of developmental arrest that represent final common morphologic pathways for a multitude of initial insults [130].

Aorticopulmonary Septation

The aorticopulmonary septum is initially formed as a condensation of mesenchyme in the roof of the aortic sac, between the fourth and sixth aortic arches (Figure 1.10) [7,130]. The extracardiac origin of this mesenchyme had been well recognized since the late 1970s [133] and in 1983 was identified by Kirby to be a population of neural crest cells [134]. Two prongs of mesenchymal condensations penetrate into the endocardial cushion ridges at the truncal end of the outflow tract. Septation moves towards the heart and is accomplished by fusion of the prongs of neural crest-derived mesenchyme. As the septum forms, the arterial trunks thus become separated by neural crest-derived smooth muscle cells [106]. As aorticopulmonary septation proceeds towards the heart and the trunks of the aorta and pulmonary artery become distinct, the distal extent of the myocardial sleeve remains at or below the septation complex. There is very little apoptosis detected in the distal

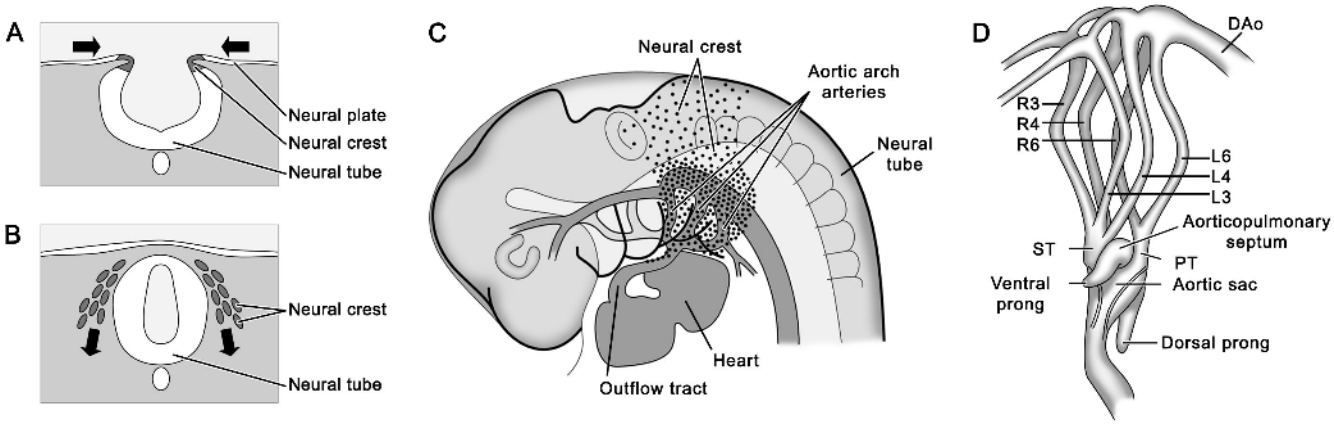

Figure 1.10 Features of the neural crest contribution to normal cardiac development. **A,** and **B,** The neural crest is a population of cells that is released to migrate throughout the embryo by fusion of the lateral neural plates to form the closed neural tube. **C,** The cardiac neural crest migrates via the aortic arch arteries into the outflow tract of the heart. **D,** The neural crest cells that form the aorticopulmonary septum form a condensed mass of cells between the fourth and sixth aortic arch vessels with two "prongs" that penetrate into the conal and truncal endocardial cushions. (PT, pulmonary trunk; ST, systemic trunk; DAo, descending aorta.) (Reproduced with permission from Kirby [130]. Contribution of neural crest to heart and vessel development. In: Harvey RP, Rosenthal N, eds. *Heart Development*. pp. 179–193. Copyright © 1999 Elsevier.)

truncal myocardium, so it is probable that the myocardium is not simply dying away [106]. It remains a topic of active debate whether subaortic conal myocardium retracts towards the heart or transdifferentiates into smooth muscle cells in the roots of the aorta and pulmonary artery [106,135,136]. In the absence of the aorticopulmonary septum, the outlet of the heart communicates with a common arterial trunk such as that seen in truncus arteriosus or in incomplete forms such as aorticopulmonary window.

Development of the Semilunar Valves

The semilunar valves develop at the juncture between the aorticopulmonary septum and the conus septum. They are derived from the parietal and septal conal ridges, the small intercalated ridges that form between the conal endocardial ridges, and the mesenchymal prongs of neural crest-derived mesenchyme that penetrate into the conal endocardial ridges. In the mouse, the neural crest cells of the mesenchymal prongs are marked by expression of the protein α-smooth muscle actin (ASMA) [106,137]. Cardiac neural crest cells can also be visualized using a variety of transgenic mouse model systems, the most frequently used being the Wnt1-cre mouse in combination with the Rosa26R-lacZ reporter mouse [67]. Fusion of the endocardial ridges occurs by contact of the ridges followed by disappearance of the endothelial cells at the site of contact. The ridges are then connected to each other by a whorl or knot-like structure of ASMA-positive cells, which is the forming aorticopulmonary septum.

Semilunar valve leaflet development begins shortly after septation. In mice, the initial process is outgrowth of unexcavated cusps of tissue corresponding to the future leaflets from the arterial surface of the distal endocardial ridges and intercalated cushions [138]. Valve sinuses are formed by active endothelial excavation of the outlet surface of the leaflets. The initial valve leaflets are thickened structures filled with an abundant extracellular ground substance densely populated with endocardial-derived mesenchymal cells bordered by a cuboidal endothelium on the arterial surface and a flattened, streamlined endothelium on the ventricular surface [139]. After the sinuses are fully excavated, the leaflets remodel into the delicate fibrous tissue characterizing mature semilunar valves [139]. Valve remodeling is a slow process that may be histologically incomplete at the time of birth [138,140]. The mechanisms of these processes are largely unexplored. The neural crest does not play as prominent a role as in aorticopulmonary septum formation – the only ASMA-positive neural crest-derived cells present in the semilunar valve leaflets as they develop are at the junctures of the leaflet commissures and the arterial wall of the great vessels [106]. These locations may hint at links between neural crest abnormalities and abnormalities of valve commissure formation or location.

A mouse model of both aortic and pulmonary valve aplasia secondary to ablation of the *Nfatc* gene has been described [141,142]. NFAT proteins are transcription factors known to be important mediators of intracellular calcium signaling in the immune system, nervous system, myocardium, and skeletal muscle [143]. NFAT signaling is initiated by calcineurin, the primary intracellular target of cyclosporine and FK506. During heart development, expression of the *Nfatc* gene is limited to a subset of cells in the endocardium, but beyond this observation the mechanism of contribution of NFATc to semilunar valve development is unknown. Although rare, aplasia of both semilunar valves has been described in humans as well [144,145]. Additionally, single semilunar valve dysplasia is one of the most common forms of congenital heart disease, either seen in isolation (e.g., bicuspid aortic valve) or in conjunction with other defects such as tetralogy of Fallot, tetralogy of Fallot with absent pulmonary valve syndrome, pulmonary atresia, and a wide variety of left ventricular outflow tract defects that include aortic valvar hypoplasia with hypoplastic left heart syndrome as its most severe manifestation.

A more complex model of abnormal semilunar valvulogenesis is found in mice deficient for *Sox4* [146]. These animals die in mid-gestation with semilunar valve insufficiency (as do NFATc-deficient embryos) and have been demonstrated to suffer from a spectrum of cardiovascular defects ranging from isolated lack of the infundibular septum to complete failure of conotruncal and aorticopulmonary septation. Additional extracardiac defects noted include tracheoesophageal fistulae. The outflow tract malformations noted in this model are hypothesized to result from abnormalities in signaling between neural crest (see below) and the outflow tract endocardial cushion cell populations. Unlike the models of common trunk associated with "pure" neural crest defects, *Sox4*-deficient mice exhibit variably severe defects in the numbers and relative differentiation of semilunar valve cusps.

Conus Septation

Formation of the conus septum is a multistep process. Initially the conal endocardial ridges are "simple" structures consisting of cardiac jelly bounded by endocardium and myocardium. As in the AV cushions, a subset of endocardial cells transdifferentiates into mesenchymal cells that then invade the cardiac jelly. The conal endocardial ridges subsequently enlarge and, with each sphincter-like contraction of the conal myocardium, are brought into apposition [93]. Fusion of the endocardial ridges, another poorly understood process, proceeds temporally from the distal conus to the base of the heart and results in an initially

mesenchymal conus septum. When the proximal conal cushions fuse they complete the separation of the subaortic and subpulmonary outflow tracts. The endocardial cushion tissue is then replaced by myocardial tissue in a process that is initially completed at the proximal conus septum and is last completed at the distal conus septum. The myocardialization of the conal cushions results in the formation of the supraventricular crest and the muscular outflow septum.

Mesenchymal neural crest prongs of the aorticopulmonary septation complex extend into the conal endocardial ridges, but unlike their role in aorticopulmonary septation they do not form the conal septum. The neural crest cells in the conal ridges disappear, possibly by an apoptotic mechanism, and their presence is speculated to be important in some way for regulating the subsequent process of myocardialization [147].

Morphogenesis of the Great Vessels and Coronary Circulation

The Neural Crest and Cardiac Development

Neural crest cells migrate into the heart through the aortic arches and are necessary for aorticopulmonary septation, outflow tract septation, and formation of the tunica media of the third, fourth, and sixth aortic arch vessels [130,134,148]. An additional population of neural crest cells differentiates into the entirety of the autonomic innervation of the heart. Other neural crest-derived structures in proximity to the developing heart and great vessels include the thymus, thyroid, and parathyroid glands.

The neural crest is a transient structure in vertebrate development originating in the dorsal-most region of the neural tube (Figure 1.10) [7,130,148,149]. The cells of the neural crest reside on the lateral margins of the neural plate and the right- and left-sided populations are brought into apposition by the folding of the neural plate into the neural tube. The cells then disperse and migrate along precise pathways to their multiple destinations. As with closure of the neural tube, this process is initiated cranially and extends caudally [148]. Specific regions of the neural crest seed cells via specific pathways to specific structures [150]. The neural crest cells that reach the outflow tract of the early heart migrate via the third, fourth, and sixth aortic arch vessels. The region of the neural crest contributing to cardiac and fourth aortic arch morphogenesis is sometimes called the "cardiac" neural crest [130,148].

Experimental ablation of the cardiac neural crest results in structural heart defects including DORV, truncus arteriosus, tetralogy of Fallot, and ventricular septal defects [149]. The most consistent impact of experimental neural crest ablation on the cardiovascular system in chick embryos is aberrant patterning of the aortic arch arteries, although no specific malformation of the aortic arch vessels is predominant in this model [130]. There are strong similarities between lesions observed following neural crest ablations in the chick embryo and the spectrum of cardiovascular anomalies in the DiGeorge syndrome [151,152]. Several cardiac teratogens in experimental animals have spectra of defects that are also comparable, such as bis-diamine in rats [153], alcohol in mice [154], nimustine hydrochloride in fetal rats and chick embryos [155,156], endothelin A blockade in chick embryos [157], and retinoic acid in humans [158]. Mouse genetic models of abnormal neural crest function include the Splotch mouse, caused by loss of the transcription factor PAX3 [159]. Endothelin signaling is particularly important in cardiac neural crest functioning, as demonstrated by the presence of aortic arch abnormalities and other neural crest-associated defects in mice bearing targeted disruptions of endothelin 1 (ET-1) [160,161], endothelin converting enzyme-1 (ECE-1) [162], and the endothelin-A (ETA) receptor [163,164]. Additional mouse models exhibiting cardiovascular features of cardiac neural crest deficiency include the trisomy 16 mouse and mice with targeted multigene deletions comparable to human chromosome 22q11 microdeletions [137,165].

Origins of the Outflow Tract Endothelium

In common with the endothelium of the aortic arch vessels, outflow tract endothelium is derived from precursors in lateral and paraxial mesoderm of the cranial region [166] corresponding to cells of the second heart field [35]. Similarly, the epicardium of the distal portion of the outflow tract is derived from a separate population of precursor cells than that of the remainder of the heart [167]. As previously noted, the outflow tract myocardium, the myocardium of the right ventricle, and interventricular septum originate from the second heart field [35]. Taken together, these data suggest a distinct developmental origin of the entirety of the cardiac outflow tract.

Epicardial Cell Migration and Development of the Coronary Arteries

The development of the epicardium is a relatively late event in the development of the heart, but its proper formation is essential for normal development of the coronary arteries, valves, and the interstitial fibroblast population of the myocardium. The epicardium migrates over the surface of the heart from villous projections in the region of the septum transversum in mammals [168–171]. The precursor tissue is histologically and functionally complex and has been called the proepicardium or proepicardial organ [172]. It is a transitory embryonic structure that gives rise to the epicardial cell layer and is also the

source of the nonmyocardial mesenchymal cells (i.e., fibroblasts, coronary smooth muscle cells) of the heart. The migrating cells eventually flatten over the surface of the myocardium and develop morphologic characteristics compatible with primitive epithelial cells. The flattening process also causes cells to occupy a greater surface area, bringing adjacent clusters of cells into contact with each other until a continuous sheet results. In the rodent, where the process is well studied, these events occur between days 9 and 11 of embryonic life, and the villous projections are markedly diminished by day 10.5 [171,172]. This is poorly understood in human development; while these important processes in rodent development are complete just before mid-gestation, in the human most are shifted towards the first 2 months of development (see [173] for comparison of developmental landmarks between human and mouse).

As the epicardial layer of cells extends over the heart, an extensive acellular extracellular matrix layer appears between the epicardium and the myocardium. If migration from the proepicardial organ is physically disrupted in chick embryos, then no epicardium develops and there is failure of the subepicardial extracellular matrix to form as well [174]. The subepicardial space becomes populated by mesenchymal subepicardial cells generally accepted to provide the precursors of cardiac fibroblasts, coronary vascular smooth muscle cells, and coronary endothelial cells. Recent publications using transgenic mouse models that allow the tracing of cells derived from the epicardium have also suggested that these cells may give rise to a population of myocytes localized in the interventricular septum [175,176]. The subepicardial extracellular matrix accumulates to its greatest degree in the AV groove. In addition to being a key site for coronary vasculogenesis, the mesenchymal cells that come to populate the AV groove matrix will form the majority of the fibrous insulating ring between the atria and the ventricles [94]. All of the cell populations just described as invading the myocardium and/or subepicardial extracellular matrix have come to be known as epicardial-derived cells (EPDCs) [97]. As identified by lineage markers, EPDCs migrate into the sulcus matrix and subsequently into the AV endocardial cushions. In addition to entering the AV cushions, EPDCs also migrate into the myocardium and subendocardium. Specific possible morphogenetic roles of the myocardial and subendocardial EPDCs have not been determined, but abnormalities of the compact myocardium, AV cushions, and coronary vasculature have all been documented in their absence [167].

The subepicardial space is the site of origin of the vascular plexus of the coronary vessel precursors. There are three sequential and overlapping phases of nutrient delivery to the myocardium during embryogenesis of the heart [109,177]. The first phase is associated with the development of an extensive network of intratrabecular sinusoids lined by endocardial cells through which nutrient flow to the myocardium likely occurs. The second phase is the development of a subepicardial plexus of endothelial-lined channels that penetrate the myocardium. A subset of these channels will communicate with the intratrabecular sinusoids. The third stage is regression and coalescence of the vascular subepicardial network into muscular arterial channels. As soon as the vessels are readily identifiable they are noted to penetrate into the ventricular and atrial walls, where they establish a mid-myocardial network. The vessels spread to the ventral surface of the heart and follow the sulci (especially the AV sulcus) to the outflow tract where they form a plexus in the myocardial sheath surrounding the truncus arteriosus. Coalescence of vessels and capillary outgrowth from the peritruncal plexus results in penetration of the wall of the aorta by the definitive proximal coronary arteries [172,177–179]. Abnormalities of this process likely contribute to the pathogenesis of a number of surgically important disease phenotypes including intramural coronary ostia, abnormalities of coronary positioning in both normally related and transposed great vessels, and anomalous left coronary artery from the pulmonary artery syndrome.

Development of the Aortic Arch

The great vessels are the conduit for blood to flow from the heart to the body and, therefore, must be formed and functional at the time of initiation of embryonic circulation (approximately day 20–22 in humans). The vessels of the embryo are formed by a process called vasculogenesis. Vasculogenesis occurs by aggregation of pre-endothelial cells (angioblasts) into networks of small endothelial channels (in contrast to the process of building vessels by sprouting growth or branching, called angiogenesis). The dorsal aorta and aortic arches are created by fusion of independently formed regional vasculogenic networks. After communications between the networks are established the definitive lumen is formed through merging of the small endothelial passages into larger channels [180,181]. The channels are functional vessels composed of only endothelial cells. Mesenchymal cells in the descending aorta and neural crest cells in the aortic arch region will then be recruited to form the smooth muscle cells of the media of the developing arteries by an obscure process [182–184]. These enveloping events require signaling through extracellular proteins known as angiopoietins via the Tie1 (TIE) and Tie2 (TEK) receptors in endothelial cells [185]. The transcription factor KLF2 (LKLF) has also been shown to be necessary for formation of the tunica media in embryonic vessels [186].

The initial embryonic arterial circulation is morphologically bilaterally symmetric and consists of multiple pairs of aortic arch vessels connecting the heart outflow to the

paired dorsal aortae. The dorsal aortae are initially paired for the full length of the embryo. Fusion of the paired aortae into a single structure begins distally and progresses retrograde to the seventh somite. As development proceeds, the paired first, second, third, fourth, and sixth aortic vessels and the dorsal aortae undergo an intricate series of transformations. The first and second aortic arch vessels regress, remaining patent only as capillary structures. The dorsal aorta between the third and fourth aortic arch vessels (the carotid duct) regresses completely, leaving no remnant, resulting in the paired third aortic arch vessels becoming the only source of blood flow from the aortic sac/truncus complex to the head of the embryo. The third aortic arch vessels become the precursors of the definitive common carotid arteries. The right dorsal aorta completely regresses at the site of dorsal aortic bifurcation; this leaves the right fourth aortic arch vessel to become a short stub connecting the right seventh intersegmental (future subclavian) artery to the aortic sac/truncus complex. The right sixth aortic arch vessel becomes the right pulmonary artery. The left sixth aortic arch vessel becomes the left pulmonary artery and the ductus arteriosus connecting the pulmonary plexus-derived distal main pulmonary artery and left pulmonary artery to the left dorsal aorta at the junction of the left dorsal aorta and the left fourth arch vessel. The left dorsal aorta remains widely patent throughout its length but remodels so that the definitive left fourth aortic arch vessel, the ductus arteriosus, and the left seventh intersegmental artery (future left subclavian artery) all connect to the left dorsal aorta within a very short span. Understanding these developmental concepts and relationships is important in planning repair of great vessel abnormalities as well as vascular rings. Despite the generally superb imaging (echocardiography, computed tomography angiography, or magnetic resonance imaging) that accompanies patients with aortic patterning defects, one is occasionally surprised by intraoperative findings. A facile knowledge of great vessel developmental derivatives can help troubleshoot an intraoperative surprise and potentially limit the dissection required to reveal the relevant operative anatomy.

The vertebral arteries are derived from anastomoses between the seven cervical intersegmental arteries. After continuity is established between the intersegmental arteries their connections to the dorsal aorta regress (with the exception of the connection of the seventh intersegmental vessel that becomes the subclavian artery) creating the subclavian origin of the definitive vertebral arteries.

Neural crest cells are critical to the normal pattern of regression or maintenance of aortic arch vessel patency (Figure 1.10) [7,130]. When neural crest cells are physically ablated in chick embryos, vascular patterning is abnormal in 100% of experiments, although the specific pattern of ablation-induced abnormalities is not predictable [181]. Neural crest cells invade and replace the original tunica media of the aortic arch vessels, but it is not known by what subsequent mechanisms neural crest cells determine the future vascular pattern.

Several genetic models of abnormal aortic vessel patterning that are not yet linked to neural crest abnormalities have been identified in mouse and zebra fish. Knockout experiments in mice involving the closely related transcription factors mesoderm/mesenchyme forkhead 1 (MF1) and mesenchyme forkhead 1 (MFH1) demonstrate cardiovascular phenotypes that include coarctation of the aorta, interruption of the aortic arch, ventricular septal defects, and in the case of MF1, thickening and partial fusion of semilunar valve leaflets [187].

Development of the Pulmonary Veins

The earliest evidence of the formation of the common pulmonary vein in the embryo is the presence of a strand of endothelial cells in the dorsal mesocardium. The endothelial strand forms a lumen and initially is a midline structure. As the dorsal mesenchymal protrusion is developing and projecting into the atrial cavity on the right side of the primitive pulmonary vein, the relative position of the pulmonary vein changes as it occupies a position to the left of the middle [67]. The continued development of the dorsal mesenchymal protrusion, the myocardialization of this mesenchyme, and the concomitant growth of the septum primum eventually result in the connection of the pulmonary vein to the left atrium in normal development [81]. Therefore, the development of the pulmonary vein does not result from an outgrowth of the atrial wall. The remodeling of the original single common pulmonary vein orifice into the four separate orifices characteristic of the mature heart is a topic deserving of additional study. Initially, the walls of the pulmonary veins are not muscular. However, as development proceeds, myocardial sleeves are formed around these veins. Recent studies have revealed some of the molecular pathways that underlie this mechanism [188]. As pulmonary myocardium is a frequent site initiating atrial fibrillation, advancing our knowledge of this event is of high importance.

Development of the Systemic Veins

The embryonic systemic veins are also formed by vasculogenesis. Initially there are three bilaterally symmetric venous drainages: the vitelline, umbilical, and cardinal venous systems [189]. The vitelline veins drain the embryonic gastrointestinal tract and gut derivatives. The umbilical veins bring oxygenated blood from the placenta to the heart. The cardinal venous system returns blood from the embryonic head, neck, and body wall. All three of these drainages enter into the sinus venosus of the primitive heart tube. The adult venous pattern is established through

complex patterns of regression, remodeling, and replacement of these embryonic venous systems and their connections to the sinus venosus [190,191].

The sinus venosus is initially bilaterally symmetric, with right and left "horns" that provide connection for the right and left common cardinal veins, umbilical veins, and vitelline veins. However, the connections of the left-sided cardinal, vitelline, and umbilical venous systems with the left horn of the sinus venosus normally regress. This results in the coronary sinus remaining as the primary structural derivative of the left horn of the sinus venosus in the normal fetal and postnatal heart. When embryonic venous connections with the left venous horn fail to regress, persistence of the left superior vena cava is observed. The right horn of the sinus venosus normally accommodates the entirety of the systemic venous drainage except the portion from the heart returned via the coronary sinus. In addition, the portion of the mature right atrium between the orifices of the vena cavae is derived from the right horn of the sinus venosus.

The right and left vitelline veins are connected to each other via a plexus of veins that become the liver sinusoids. The left vitelline vein regresses after it loses connection with the left horn of the sinus venosus. Therefore, the entire venous system of the embryonic gut normally drains to the heart through the right vitelline vein. The connection of the right vitelline vein to the right sinus venosus persists into fetal and adult life as the terminal portion of the inferior vena cava.

The left umbilical vein also loses its connection with the left horn of the sinus venosus, but it is the right umbilical vein that regresses as a distinct structure. The left umbilical vein forms anastomoses with the ductus venosus (derived from the liver plexus of the vitelline veins). No derivatives of the embryonic umbilical venous drainage connect to the heart or persist following the closure of the ductus venosus in adult life.

The cardinal venous system initially consists of bilateral anterior cardinal veins and bilateral posterior cardinal veins. Fusion of the anterior and posterior cardinal veins at the level of the sinus venosus forms the common cardinal veins. The left anterior cardinal vein loses its connection with the left horn of the sinus venosus, but a small remnant on the surface of the heart normally persists as a passage of coronary venous blood to the coronary sinus and is known as the oblique vein of the left atrium. Another portion of the left anterior cardinal vein persists as the left internal jugular vein. As the left anterior cardinal vein loses connection with the heart it becomes connected to the right anterior cardinal vein via the intercardinal anastomosis that forms between the thyroid vein and the thymic vein; this connection will persist as the left brachiocephalic vein. The portion of the right anterior cardinal vein between the right atrium and the drainage of the left anterior cardinal vein proximally (via the intercardinal anastomosis) becomes the normal right superior vena cava.

The posterior cardinal veins are the only portions of the embryonic venous drainage that are destined to have a symmetrical fate. Both posterior cardinal veins will regress throughout most of their length and lose their direct connections with the sinus venosus. The posterior cardinal veins originally drain the body wall, gonadal, and renal structures. Their function in venous drainage of the body wall is supplanted by the supracardinal venous plexus, while the gonadal and renal venous drainage is captured by the subcardinal venous plexus.

The posterior cardinal, supracardinal, and subcardinal venous beds contribute the segments that form the definitive inferior vena cava (IVC) to the level of the vitelline vein-derived segment connecting to the right atrium origin. Remnants of the posterior cardinal veins in the fetal and adult circulation are limited to the most distal portion of the IVC (formed by anastomosis of the right and left posterior cardinal veins) and the common iliac veins. The posterior cardinal vein-derived IVC connects to the supracardinal segment of the IVC. The supracardinal venous system is the site of origin of the azygous and hemiazygous veins, which ordinarily connect to the IVC between the renal veins and the common iliac veins. The supracardinal segment of the IVC connects to the subcardinal segment of the IVC, which receives the drainage of the gonadal veins and renal veins before connecting to the vitelline venous channel into the heart.

In both the supracardinal and subcardinal venous systems the initial vascular structures are bilaterally symmetric, with the left-sided channels regressing and the right-sided channels persisting, resulting in the typical right sided location of the IVC. The mechanisms through which the definitive systemic venous structures are formed are very poorly understood. The frequency of venous drainage abnormalities in human and animal models of altered left-right axis differentiation [73] makes it clear that the mechanisms of venous morphogenesis are likely dependent on appropriate left-right signaling. This is a particularly important series of developmental relationship that persists in those cases of interrupted IVC with azygous continuation in which the hepatic veins drain directly into the right atrium.

References

1. Hamburger V, Hamilton HL. (1992) A series of normal stages in the development of the chick embryo. 1951. Dev Dyn 195, 231–272.
2. O'Rahilly R, Muller F, Streeter GL. (1987) *Developmental Stages in Human Embryos*. Washington, DC: Carnegie Institution of Washington.
3. Streeter GL. (1942) Developmental horizons in human embryos. Description of age group XI, 13–20 somites, and

age group XII, 21–29 somites. Contrib Embryol 30, 211–245.
4. Streeter GL. (1945) Developmental horizons in human embryos. Description of age group XIII, embryos about 4 or 5 millimeters long, and age group XIV, period of indentation of lens cesicle. Contrib Embryol 32, 27–63.
5. Streeter GL. (1948) Developmental horizons in human embryos. Description of age group XI, 13–20 somites, age group XV, XVI, XVII, and XVII. Contrib Embryol 32, 133–203.
6. Theiler K. (1989) *The House Mouse: Atlas of Embryonic Development*. New York, NY: Springer Verlag.
7. McQuinn T, Wessels A. (2003) Embryology of the heart and great vessels. In: Mavroudis C, Backer CL, editors. *Pediatric Cardiac Surgery* 3rd ed. Philadelphia, PA: Mosby Inc. pp. 1–24.
8. Gilbert SF. (1994) *Developmental Biology*. Sunderland, MA: Sinauer Associates Inc. pp. 202–243.
9. Inagaki T, Garcia-Martinez V, Schoenwolf GC. (1993) Regulative ability of the prospective cardiogenic and vasculogenic areas of the primitive streak during avian gastrulation. Dev Dyn 197, 57–68.
10. Lough J, Sugi Y. (2000) Endoderm and heart development. Dev Dyn 217, 327–342.
11. Black BL, Olson E. (1999) Control of cardiac development by the MEF2 family of transcription factors. In: Harvey M, Rosenthal N, editors. *Heart Development*. San Diego, CA: Academic Press. pp. 131–142.
12. Bruneau BG, Logan M, Davis N, *et al*. (1999) Chamber-specific cardiac expression of Tbx5 and heart defects in Holt–Oram syndrome. Dev Biol 211, 100–108.
13. Harvey RP, Biben C, Elliott DA. (1999) Transcriptional control and pattern formation in the developing vertebrate heart: Studies on NK-2 class homeodomain factors. In: Harvey RP, Rosenthal N, editors. *Heart Development*. San Diego, CA: Academic Press. pp. 111–129.
14. Horb ME, Thomsen GH. (1999) Tbx5 is essential for heart development. Development 126, 1739–1751.
15. Parmacek MS. (1999) GATA transcription factors and cardiac development. In: Harvey M, Rosenthal N, editors. *Heart Development*. San Diego, CA: Academic Press. pp. 291–306.
16. Srivastava D. (1999) Segmental regulation of cardiac development by the basic helix-loop-helix transcription factors dHAND and eHAND. In: Harvey M, Rosenthal N, editors. *Heart Development*. San Diego, CA: Academic Press. pp. 143–155.
17. Prall OW, Menon MK, Solloway MJ, *et al*. (2007) An Nkx2-5/Bmp2/Smad1 negative feedback loop controls heart progenitor specification and proliferation. Cell 128, 947–959.
18. Mohun TJ, Leong LM. (1999) Heart formation and the heart field in amphibian embryos. In: Harvey M, Rosenthal N, editors. *Heart Development*. San Diego, CA: Academic Press. pp. 37–49.
19. Baldwin HS, Jensen KL, Solursh M. (1991) Myogenic cytodifferentiation of the precardiac mesoderm in the rat. Differentiation 47, 163–172.
20. Goss CM (1942) The physiology of the embryonic mammalian heart before circulation. Am J Physiol 137, 146–152.
21. Linask KK, Lash JW (1988) A role for fibronectin in the migration of avian precardiac cells. I. Dose-dependent effects of fibronectin antibody. Dev Biol 129, 315–323.
22. De Ruiter M, Poelmann R, VanderPlas-de Vries I, *et al.* (1992) The development of the myocardium and endocardium in mouse embryos. Anat Embryol 185, 461–473.
23. De Haan RL. (1959) Cardia bifida and the development of pacemaker function in the early chicken heart. Dev Biol 1, 586–602.
24. Webb S, Brown NA, Anderson RH, *et al*. (2000) Relationship in the chick of the developing pulmonary vein to the embryonic systemic venous sinus. Anat Rec 259, 67–75.
25. Snarr BS, O'Neal JL, Chintalapudi MR, *et al*. (2007) Isl1 expression at the venous pole identifies a novel role for the second heart field in cardiac development. Circ Res 101, 971–974.
26. Snarr BS, Wirrig EE, Phelps AL, *et al*. (2007) A spatiotemporal evaluation of the contribution of the dorsal mesenchymal protrusion to cardiac development. Dev Dyn 236, 1287–1294.
27. Verberne ME, Gittenberger-de Groot AC, van Iperen L, *et al*. (2000) Distribution of different regions of cardiac neural crest in the extrinsic and the intrinsic cardiac nervous system. Dev Dyn 217, 191–204.
28. Sohal GS, Ali MM, Ali AA, *et al*. (1999) Ventrally emigrating neural tube cells differentiate into heart muscle. Biochem Biophys Res Comm 254, 601–604.
29. Rawles ME. (1943) The heart-forming ares of the early chick blastoderm. Physiol Zool 16, 22–42.
30. Rosenquist GC, De Haan RL. (1966) Migration of precardiac cells in the chick embryo: a radioautographic study. *Contributions to Embryology*. Washington, DC: Carnegie Institute of Washington. pp. 111–121.
31. Stalsberg H, DeHaan RL. (1969) The precardiac areas and formation of the tubular heart in the chick embryo. Dev Biol 19, 128–159.
32. de la Cruz MV, Sanchez Gomez C, Arteaga MM, *et al.* (1977) Experimental study of the development of the truncus and the conus in the chick embryo. J Anat 123, 661–686.
33. Kelly RG, Brown NA, Buckingham ME. (2001) The arterial pole of the mouse heart forms from Fgf10-expressing cells in pharyngeal mesoderm. Dev Cell 1, 435–440.
34. Mjaatvedt CH, Nakaoka T, Moreno-Rodriguez R, *et al.* (2001) The outflow tract of the heart is recruited from a novel heart-forming field. Dev Biol 238, 97–109.
35. Verzi MP, McCulley DJ, De Val S, *et al.* (2005) The right ventricle, outflow tract, and ventricular septum comprise a restricted expression domain within the secondary/anterior heart field. Dev Biol 287, 134–145.
36. Waldo KL, Kumiski DH, Wallis KT, *et al.* (2001) Conotruncal myocardium arises from a secondary heart field. Development 128, 3179–3188.
37. de la Cruz MV, Sanchez-Gomez C, Palomino MA. (1989) The primitive cardiac regions in the straight tube heart (Stage 9) and their anatomical expression in the mature heart: an experimental study in the chick embryo. J Anat 165, 121–131.
38. Patten BM, Kramer TC. (1933) The initiation of contraction in the embryonic chick heart. Am J Anatomy 53, 349–375.

39. Castro-Quezada A, Nadal-Ginard B, de la Cruz MV. (1972) Experimental study of the formation of the bulboventricular loop in the chick. J Embryol Exp Morphol 27, 623–637.
40. Markwald RR, Trusk T, Moreno-Rodriguez R. (1998) Formation and septation of the tubular heart integrating the dynamics of morphology with emerging molecular concepts. In: de la Cruz MV, Markwald RR, editors. *Living Morphogenesis of the Heart*. Boston, MA: Birkhauser. pp. 43–84.
41. Moorman AF, Lamers WH. (1998) Molecular anatomy of the developing heart. Trends Cardiovasc Med 4, 257–264.
42. de Jong F, Opthof T, Wilde AA, *et al.* (1992) Persisting zones of slow impulse conduction in developing chicken hearts. Circ Res 71, 240–250.
43. Conlon RA, Rossant J. (1992) Exogenous retinoic acid rapidly induces anterior ectopic expression of murine Hox-2 genes in vivo. Development 116, 357–368.
44. Ruiz i Altaba A, Jessell T. (1991) Retinoic acid modifies mesodermal patterning in early *Xenopus* embryos. Genes Dev 5, 175–187.
45. Conlon RA. (1995) Retinoic acid and pattern formation in vertebrates. Trends Genet 8, 314–319.
46. Kastner P, Grondona JM, Mark M, *et al.* (1994) Genetic analysis of RXRα developmental function: convergence of RXR and RAR signaling pathways in heart and eye morphogenesis. Cell 78, 987–1003.
47. Osmond MK, Butler AJ, Voon FCT, *et al.* (1991) The effects of retinoic acid on heart formation in the early chick embryo. Development 113, 1405–1417.
48. Smith S, Dickman ED. (1997) New insights into retinoid signaling in cardiac development and physiology. Trends Cardiovasc Med 7, 324–329.
49. Gruber PJ, Kubalak SW, Pexieder T, *et al*. (1996) RXRα deficiency confers genetic susceptibility for aortic sac, conotruncal, atrioventricular cushion, and ventricular muscle defects in mice. J Clin Invest 98, 1332–1343.
50. Dersch H, Zile MH. (1993) Induction of normal cardiovascular development in the vitamin A-deprived quail embryo by natural retinoids. Dev Biol 160, 424–433.
51. Heine UI, Roberts AB, Munoz EF, *et al.* (1985) Effects of retinoid deficiency on the development of the heart and vascular system of the quail embryo. Virchows Archives (Cell Pathology) 50, 135–152.
52. Twal W, Roze L, Zile MH. (1995) Anti-retinoic acid monoclonal antibody localizes all-trans-retinoic acid in target cells and blocks normal development in early quail embryo. Dev Biol 168, 225–234.
53. Dickman ED, Smith SM. (1996) Selective regulation of cardiomyocyte gene expression and cardiac morphogenesis by retinoic acid. Dev Dyn 206, 39–48.
54. Pexieder T, Blanc O, Pelouch V, *et al*. (1995) Late fetal development of retinoic acid induced transposition of the great arteries. In: Clark MR, Takas A, editors. *Developmental Mechanisms of Heart Disease*. Armonk, NY: Futura Publishing Company. pp. 297–307.
55. Kostetskii I, Jiang Y, Kostetskaia E, *et al.* (1999) Retinoid signaling required for normal heart development regulates GATA-4 in a pathway distinct from cardiomyocyte differentiation. Dev Biol 206, 206–218.
56. Liberatore CM, Searcy-Schrick RD, Yutzey KE. (2000) Ventricular expression of tbx5 inhibits normal heart chamber development. Dev Biol 223, 169–180.
57. Yutzey KE, Rhee JT, Bader D. (1994) Expression of the atrial-specific myosin heavy chain AMHC1 and the establishment of anterior polarity in the developing chicken heart. Development 120, 871–883.
58. Means A, Gudas L. (1995) The roles of retinoids in vertebrate development. Annu Rev Biochem 64, 201–233.
59. Moss JB, Xavier-Neto J, Shapiro MD, *et al.* (1998) Dynamic patterns of retinoic acid synthesis and response in the developing mammalian heart. Dev Biol 199, 55–71.
60. Xavier-Neto J, Shapiro MD, Houghton L, *et al.* (2000) Sequential programs of retinoic acid synthesis in the myocardial and epicardial layers of the developing avian heart. Dev Biol 219, 129–141.
61. Kelly RG, Franco D, Moorman AF, *et al.* (1999) Regionalization of transcriptional potential in the myocardium. In: Harvey RP, Rosenthal N, editors. *Heart Development*. San Diego, CA: Academic Press. pp. 333–355.
62. He CZ, Burch JB. (1997) The chicken GATA-6 locus contains multiple control regions that confer distinct patterns of heart region-specific expression in transgenic mouse embryos. J Biol Chem 272, 28550–28556.
63. Srivastava D, Thomas T, Lin Q, *et al.* (1997) Regulation of cardiac mesodermal and neural crest development by the bHLH transcription factor, dHAND. Nat Gen 16, 154–160.
64. Akagi K, Sandig V, Vooijs M, *et al.* (1997) Cre-mediated somatic site-specific recombination in mice. Nucleic Acids Res 25, 1766–1773.
65. McCulley DJ, Kang JO, Martin JF, *et al.* (2008) BMP4 is required in the anterior heart field and its derivatives for endocardial cushion remodeling, outflow tract septation, and semilunar valve development. Dev Dyn 237, 3200–3209.
66. Moon A. (2008) Mouse models of congenital cardiovascular disease. Cur Top Dev Biol 84, 171–248.
67. Snarr BS, Kern CB, Wessels A. (2008) Origin and fate of cardiac mesenchyme. Dev Dyn 237, 2804–2819.
68. Manner J. (2000) Cardiac looping in the chick embryo: A morphological review with special reference to terminological and biomechanical aspects of the looping process. Anat Rec 259, 248–262.
69. Manner J. (2009) The anatomy of cardiac looping: a step towards the understanding of the morphogenesis of several forms of congenital cardiac malformations. Clin Anat 22, 21–35.
70. Yost HJ. (1999) Establishing cardiac left-right asymmetry. In: Harvey RP, Rosenthal N, editors. *Heart Development*. San Diego, CA: Academic Press. pp. 373–389.
71. Bakkers J, Verhoeven MC, Abdelilah-Seyfried S. (2009) Shaping the zebrafish heart: from left-right axis specification to epithelial tissue morphogenesis. Dev Biol 330, 213–220.
72. Meyers EN, Martin GR. (1999) Differences in left–right axis pathways in mouse and chick: functions of FGF8 and SHH. Science 285, 403–406.
73. McQuinn TC, Miga DE, Mjaatvedt CH, *et al.* (2001) Cardiopulmonary malformations in the inv/inv mouse. Anat Rec 263, 62–71.

74. Icardo JM, Sanchez de Vega MJ. (1991) Spectrum of heart malformations in mice with situs solitus, situs inversus, and associated visceral heterotaxy. Circulation 84, 2547–2558.
75. Layton WM, Jr. (1976) Random determination of a developmental process: reversal of normal visceral asymmetry in the mouse. J Hered 67, 336–338.
76. Yokoyama T, Copeland NG, Jenkins NA, *et al.* (1993) Reversal of left-right asymmetry: a situs inversus mutation. Science 260, 679–682.
77. Tan SY, Rosenthal J, Zhao XQ, *et al*. (2007) Heterotaxy and complex structural heart defects in a mutant mouse model of primary ciliary dyskinesia. J Clin Invest 117, 3742–3752.
78. Casey B, Hackett BP. (2000) Left–right axis malformations in man and mouse. Curr Opin Genet Dev 10, 257–261.
79. Franco D, Kelly R, Lamers WH, *et al.* (1997) Regionalized transcriptional domains of myosin light chain 3f transgenes in the embryonic mouse heart: morphogenetic implications. Dev Biol 188, 17–33.
80. Kitamura K, Miura H, Miyagawa-Tomita S, *et al.* (1999) Mouse Pitx2 deficiency leads to anomalies of the ventral body wall, heart, extra- and periocular mesoderm and right pulmonary isomerism. Development 126, 5749–5758.
81. Wessels A, Anderson RH, Markwald RR, *et al.* (2000) Atrial development in the human heart: an immunohistochemical study with emphasis on the role of mesenchymal tissues. Anat Rec 259, 288–300.
82. Manasek FJ, Monroe RG. (1972) Early cardiac morphogenesis is independent of function. Dev Biol 27, 584–588.
83. Manning A, McLachlan JC. (1990) Looping of chick embryo hearts in vitro. J Anat 168, 257–263.
84. Taber LA. (2006) Biophysical mechanisms of cardiac looping. Int J Dev Biol 50, 323–332.
85. Sissman NJ. (1966) Cell multiplication rates during development of the primitive cardiac tube in the chick embryo. Nature 210, 504–507.
86. Stalsberg H. (1969) The origin of heart asymmetry: right and left contributions to the early chick embryo heart. Dev Biol 19, 109–127.
87. Itasaki N, Nakamura H, Sumida H, *et al.* (1991) Actin bundles on the right side in the caudal part of the heart tube play a role in dextro-looping in the embryonic chick heart. Anat Embryol (Berl) 183, 29–39.
88. Mjaatvedt CH, Yamamura H, Wessels A, *et al.* (1999) Mechanisms of segmentation, septation, and remodeling of the tubular heart: endocardial cushion fate and cardiac looping. In: Harvey RP, Rosenthal N, editors. *Heart Development*. San Diego, CA: Academic Press. pp. 159–175.
89. van den Hoff MJ, Moorman AF, Ruijter JM, *et al.* (1999) Myocardialization of the cardiac outflow tract. Dev Biol 212, 477–490.
90. Davis CL. (1924) The cardiac jelly of the chick embryo. Anat Rec 27, 201.
91. Kitten GT, Markwald RR, Bolender DL. (1987) Distribution of basement membrane antigens in cryopreserved early embryonic hearts. Anat Rec 217, 379–390.
92. Markwald RR, Krug EL, Runyan RB, *et al.* (1985) Proteins in cardiac jelly which induce mesenchyme formation. In: Ferrans VA, Rosenquist GC, Weinstein C, editors. *Cardiac Morphogenesis*. New York, NY: Elsevier. pp. 60–68.
93. Patten BM, Kramer TC, Barry A. (1948) Valvular action in the embryonic chick heart by localized apposition of endocardial masses. Anat Rec 102, 299–311.
94. Wessels A, Markman MW, Vermeulen JL, *et al.* (1996) The development of the atrioventricular junction in the human heart. Circ Res 78, 110–117.
95. Van Mierop LH, Alley RD, Kausel HW, *et al.* (1962) The anatomy and embryology of endocardial cushion defects. J Thorac Cardiovasc Surg 43, 71–83.
96. Bolender DL, Markwald RR. (1979) Epithelial–mesenchymal transformation in chick atrioventricular cushion morphogenesis. Scan Electron Microsc, 313–321.
97. Gittenberger-de Groot AC, Vrancken Peeters MP, Mentink MM, *et al.* (1998) Epicardium-derived cells contribute a novel population to the myocardial wall and the atrioventricular cushions. Circ Res 82, 1043–1052.
98. Fitzharris TP. (1981) Endocardial shape change in the truncus during cushion tissue formation. In: Pexieder T, editor. *Mechanisms of Cardiac Morphogenesis and Teratogenesis*. New York, NY: Raven Press. pp. 227–235.
99. Markwald RR, Fitzharris TP, Manasek FJ. (1977) Structural development of endocardial cushions. Am J Anat 148, 85–120.
100. Pexieder T. (1981) Prenatal development of the endocardium: a review. Scan Electron Microsc, 223–253.
101. Nakajima Y, Krug EL, Markwald RR. (1994) Myocardial regulation of transforming growth factor-beta expression by outflow tract endothelium in the early embryonic chick heart. Dev Biol 165, 615–626.
102. Nakajima Y, Yamagishi T, Nakamura H, *et al.* (1998) An autocrine function for transforming growth factor (TGF)-β3 in the transformation of atrioventricular canal endocardium into mesenchyme during chick heart development. Dev Biol 194, 99–113.
103. Runyan RB, Markwald RR. (1983) Invasion of mesenchyme into three-dimensional collagen gels: a regional and temporal analysis of interaction in embryonic heart tissue. Dev Biol 95, 108–114.
104. De Ruiter MC, Poelmann RE, VanMunsteren JC, *et al.* (1997) Embryonic endothelial cells transdifferentiate into mesenchymal cells expressing smooth muscle actins in vivo and in vitro. Circ Res 80, 444–451.
105. Lamers WH, Virágh S, Wessels A, *et al.* (1995) Formation of the tricuspid valve in the human heart. Circulation 91, 111–121.
106. Ya J, Vandenhoff MJB, Deboer PAJ, *et al*. (1998) Normal development of the outflow tract in the rat. Circ Res 82, 464–472.
107. Sedmera D, Pexieder T, Vuillemin M, *et al.* (2000) Developmental patterning of the myocardium. Anat Rec 258, 319–337.
108. Challice CE, Viragh S. (1974) The architectural development of the early mammalian heart. Tissue Cell 6, 447–462.
109. Tokuyasu KT. (1985) Development of myocardial circulation. In: Ferrans VJ, Rosenquist G, Weinstein C, editors. *Cardiac Morphogenesis*. Amsterdam, Netherlands: Elsevier. pp. 226–237.
110. Hogers B, DeRuiter MC, Baasten AM, *et al.* (1995) Intracardiac blood flow patterns related to the yolk sac circulation of the chick embryo. Circ Res 76, 871–877.

111. Wessels A, Vermeulen JL, Verbeek FJ, *et al.* (1992) Spatial distribution of "tissue-specific" antigens in the developing human heart and skeletal muscle. III. An immunohistochemical analysis of the distribution of the neural tissue antigen G1N2 in the embryonic heart; implications for the development of the atrioventricular conduction system. Anat Rec 232, 97–111.
112. Moorman AFM, Lamers WH. (1999) Development of the conduction system of the vertebrate heart. In: Harvey RP, Rosenthal N, editors. *Heart Development*. San Diego, CA: Academic Press. pp. 195–207.
113. Lamers WH, Wessels A, Verbeek FJ, *et al.* (1992) New findings concerning ventricular septation in the human heart. Implications for maldevelopment. Circulation 86, 1194–1205.
114. de la Cruz MV, Markwald RR. (1998) Embryological development of the ventricular inlets: septation and atrioventricular valve apparatus. In: de la Cruz MV, Markwald RR, editors. *Living Morphogenesis of the Heart*. Boston, MA: Birkhauser. pp. 131–155.
115. Manner J. (1999) Does the subepicardial mesenchyme contribute myocardioblasts to the myocardium of the chick embryo heart? A quail-chick chimera study tracing the fate of the epicardial primordium. Anat Rec 255, 212–226.
116. Wessels A, Mijnders TA, de Gier-de Vries C, *et al.* (1992) Expression of myosin heavy chain in neonate human hearts. Cardiol Young 2, 318–334.
117. Anderson RH, Becker AE, Brachenmacher C, *et al.* (1972) Ventricular preexcitation: a proposed nomenclature for its substrates. Euro J Cardiol 3, 27–36.
118. Oosthoek PW, Wenink AC, Vrolijk BC, *et al.* (1998) Development of the atrioventricular valve tension apparatus in the human heart. Anat Embryol (Berl) 198, 317–329.
119. Oosthoek PW, Wenink AC, Wisse LJ, *et al.* (1998) Development of the papillary muscles of the mitral valve: morphogenetic background of parachute-like asymmetric mitral valves and other mitral valve anomalies. J Thorac Cardiovasc Surg 116, 36–46.
120. Van Mierop LH, Gessner IH. (1970) The morphologic development of the sinoatrial node in the mouse. Am J Cardiol 25, 204–212.
121. Domenech-Mateu JM, Arno-Palau A, Martinez-Pozo A. (1991) Study of the development of the atrioventricular conduction system as a consequence of observing an extra atrioventricular node in the normal heart of a human fetus. Anat Rec 230, 73–85.
122. Cheng G, Litchenberg WH, Cole GJ, *et al.* (1999) Development of the cardiac conduction system involves recruitment within a multipotent cardiomyogenic lineage. Development 126, 5041–5049.
123. Gourdie RG, Mima T, Thompson RP, *et al.* (1995) Terminal diversification of the myocyte lineage generates Purkinje fibers of the cardiac conduction system. Development 121, 1423–1431.
124. Moorman AF, de Jong F, Denyn MM, *et al.* (1998) Development of the cardiac conduction system. Circ Res 82, 629–644.
125. Viragh S, Challice CE. (1973) The impulse generation and conduction system of the heart. In: Challice CE, Viragh S, editors. *Ultrastructure of the Mammalian Heart*. New York, NY: Academic Press. pp. 43–89.
126. Canale E, Smolich JJ, Campbell GR. (1987) Differentiation and innervation of the atrioventricular bundle and ventricular Purkinje system in sheep heart. Development 100, 641–651.
127. Gourdie RG, Wei Y, Kim D, *et al.* (1998) Endothelin-induced conversion of embryonic heart muscle cells into impulse-conducting Purkinje fibers. Proc Natl Acad Sci U S A 95, 6815–6818.
128. Pexieder T (1995) Overview: conotruncus and its septation at the advent of the molecular biology era. In: Clark EB, Markwald RR, Takao A, editors. *Developmental Mechanisms of Heart Disease*. Armonk, NY: Futura Publishing Co., Inc. pp. 227–247.
129. Gittenberger-de Groot AC, Poelmann RE. (1997) Principles of abnormal cardiac development. In: Burggren W, Keller B, editors. *Development of Cardiovascular Systems*. New York, NY: University Press. pp. 259–267.
130. Kirby ML. (1999) Contribution of neural crest to heart and vessel development. In: Harvey RP, Rosenthal N, editors. *Heart Development*. San Diego, CA: Academic Press. pp. 179–193.
131. Hogers B, DeRuiter MC, Gittenberger-de Groot AC, *et al.* (1997) Unilateral vitelline vein ligation alters intracardiac blood flow patterns and morphogenesis in the chick embryo. Circ Res 80, 473–481.
132. Hogers B, DeRuiter MC, Gittenberger-de Groot AC, *et al.* (1999) Extraembryonic venous obstructions lead to cardiovascular malformations and can be embryolethal. Cardiovasc Res 41, 87–99.
133. Thompson RP, Fitzharris TP. (1979) Morphogenesis of the truncus arteriosus of the chick embryo heart: the formation and migration of mesenchymal tissue. Am J Anat 154, 545–556.
134. Kirby ML, Gale TF, Stewart DE. (1983) Neural crest cells contribute to normal aorticopulmonary septation. Science 220, 1059–1061.
135. Bartelings MM, Gittenberger-de Groot AC. (1988) The arterial orifice level in the early human embryo. Anat Embryol (Berl) 177, 537–542.
136. Thompson RP, Fitzharris TP. (1985) Division of cardiac flow. In: Ferrans VA, Rosenquist GC, Weinstein C, editors. *Cardiac Morphogenesis*. New York, NY: Elsevier. pp. 169–180.
137. Waller BR, McQuinn T, Phelps AL, *et al.* (2000) Conotruncal anomalies in the Trisomy 16 mouse: an immunohistochemical analysis with emphasis on the involvement of neural crest. Anat Rec 260, 279–293.
138. Hurle JM, Colvee E, Blanco AM. (1980) Development of mouse semilunar valves. Anat Embryol (Berl) 160, 83–91.
139. Maron BJ, Hutchins GM. (1974) The development of the semilunar valves in the human heart. Am J Pathol 74, 331–344.
140. Hyams VJ, Manion WC. (1968) Incomplete differentiation of the cardiac valves. A report of 197 cases. Am Heart J 76, 173–182.
141. de la Pompa JL, Timmerman LA, Takimoto H, *et al.* (1998) Role of the NF-ATc transcription factor in morphogenesis of cardiac valves and septum. Nature 392, 182–186.

142. Ranger AM, Grusby MJ, Hodge MR, *et al.* (1998) The transcription factor NF-ATc is essential for cardiac valve formation. Nature 392, 186–190.
143. Crabtree GR (1999) Generic signals and specific outcomes: signaling through Ca2+, calcineurin, and NF-AT. Cell 96, 611–614.
144. Hartwig NG, Vermeij-Keers C, De Vries HE, *et al.* (1991) Aplasia of semilunar valve leaflets: two case reports and developmental aspects. Pediatric Cardiol 12, 114–117.
145. Miyabara S, Ando M, Yoshida K, *et al.* (1994) Absent aortic and pulmonary valves: investigation of three fetal cases with cystic hygroma and review of the literature. Heart Vessels 9, 49–55.
146. Ya J, Schilham MW, de Boer PA, *et al.* (1998) Sox4-deficiency syndrome in mice is an animal model for common trunk. Circ Res 83, 986–994.
147. Poelmann RE, Mikawa T, Gittenberger-de Groot AC. (1998) Neural crest cells in outflow tract septation of the embryonic chicken heart: differentiation and apoptosis. Dev Dyn 212, 373–384.
148. Gilbert SF. (1994) *Developmental Biology* 4th ed. Sunderland, MA: Sinauer Associates Inc. pp. 272–288.
149. Kirby ML, Turnage KL 3rd, Hays BM. (1985) Characterization of conotruncal malformations following ablation of "cardiac" neural crest. Anat Rec 213, 87–93.
150. Phillips MT, Kirby ML, Forbes G. (1987) Analysis of cranial neural crest distribution in the developing heart using quail-chick chimeras. Circ Res 60, 27–30.
151. Nishibatake M, Kirby ML, Van Mierop LH. (1987) Pathogenesis of persistent truncus arteriosus and dextroposed aorta in the chick embryo after neural crest ablation. Circulation 75, 255–264.
152. Van Mierop LH, Kutsche LM. (1986) Cardiovascular anomalies in DiGeorge syndrome and importance of neural crest as a possible pathogenetic factor. Am J Cardiol 58, 133–137.
153. Ikeda T, Matsuo T, Kawamoto K, *et al.* (1984) Bis-diamine induced defects of the branchial apparatus in rats. In: Nora JJ, Takao A, editors. *Congenital Heart Disease: Causes and Processes*. Mt Kisco, NY: Futura. pp. 223–236.
154. Daft PA, Johnston MC, Sulik KK. (1986) Abnormal heart and great vessel development following acute ethanol exposure in mice. Teratology 33, 93–104.
155. Miyagawa S, Ando M, Takao A. (1988) Cardiovascular anomalies produced by nimustine hydrochloride in the rat fetus. Teratology 38, 553–558.
156. Miyagawa S, Kirby ML. (1989) Pathogenesis of persistent truncus arteriosus induced by nimustine hydrochloride in chick embryos. Teratology 39, 287–294.
157. Kempf H, Linares C, Corvol P, *et al*. (1998) Pharmacological inactivation of the endothelin type A receptor in the early chick embryo: a model of mispatterning of the branchial arch derivatives. Development 125, 4931–4941.
158. Lammer E, Chen D, Hoar R, *et al.* (1985) Retinoic acid embryopathy. N Engl J Med 313, 837–841.
159. Conway SJ, Henderson DJ, Copp AJ. (1997) Pax3 is required for cardiac neural crest migration in the mouse: evidence from the *splotch* (*Sp^{2H}*) mutant. Development 124, 505–514.
160. Kurihara Y, Kurihara H, Oda H, *et al.* (1995) Aortic arch malformations and ventricular septal defects in mice deficient in endothelin-1. J Clin Invest 96, 293–300.
161. Yanagisawa H, Hammer RE, Richardson JA, *et al.* (1998) Role of endothelin-1/endothelin-A receptor-mediated signaling pathway in the aortic arch patterning in mice. J Clin Invest 102, 22–33.
162. Yanagisawa H, Yanagisawa M, Kapur RP, *et al.* (1998) Dual genetic pathways of endothelin-mediated intercellular signaling revealed by targeted disruption of endothelin converting enzyme-1 gene. Development 125, 825–836.
163. Clouthier DE, Hosoda K, Richardson JA, *et al*. (1998) Cranial and cardiac neural crest defects in endothelin-A receptor-deficient mice. Development 125, 813–824.
164. Clouthier DE, Williams SC, Yanagisawa H, *et al.* (2000) Signaling pathways crucial for craniofacial development revealed by endothelin-A receptor-deficient mice. Dev Biol 217, 10–24.
165. Lindsay EA, Botta A, Jurecic V, *et al.* (1999) Congenital heart disease in mice deficient for the DiGeorge syndrome region. Nature 401, 379–383.
166. Noden DM. (1991) Origins and patterning of avian outflow tract endocardium. Development 111, 867–876.
167. Gittenberger-de Groot AC, Peeters M, Bergwerff M, *et al.* (2000) Epicardial outgrowth inhibition leads to compensatory mesothelial outflow tract collar and abnormal cardiac septation and coronary formation. Circ Res 87, 969–971.
168. Ho E, Shimada Y. (1978) Formation of the epicardium studied with the scanning electron microscope. Dev Biol 66, 579–585.
169. Shimada Y, Ho E. (1980) Scanning electron microscopy of the embryonic chick heart: formation of the epicaridium and surface structure of the four heterotypic cells that constitute the embryonic heart. In: Van Praagh R, Takao A, editors. *Etiology and Morphogenesis of Congenital Heart Disease*. Mt Kisco, NY: Futura.
170. Shimada Y, Ho E, Toyota N. (1981) Epicardial covering over myocardial wall in the chicken embryo as seen with the scanning electron microscope. Scan Electr Microsc, 275–280.
171. Komiyama M, Ito K, Shimada Y. (1987) Origin and development of the epicardium in the mouse embryo. Anat Embryol 176, 183–189.
172. Viragh S, Gittenberger-de Groot AC, Poelmann RE, *et al.* (1993) Early development of quail heart epicardium and associated vascular and glandular structures. Anat Embryol (Berl) 188, 381–393.
173. Sissman NJ. (1970) Developmental landmarks in cardiac morphogenesis: comparative chronology. Am J Cardiol 25, 141–148.
174. Manner J. (1993) Experimental study on the formation of the epicardium in chick embryos. Anat Embryol 187, 281–289.
175. Cai CL, Martin JC, Sun Y, *et al.* (2008) A myocardial lineage derives from Tbx18 epicardial cells. Nature 454, 104–108.
176. Zhou B, Ma Q, Rajagopal S, *et al.* (2008) Epicardial progenitors contribute to the cardiomyocyte lineage in the developing heart. Nature 454, 109–113.

177. Waldo KL, Willner W, Kirby ML. (1990) Origin of the proximal coronary artery stems and a review of ventricular vascularization in the chick embryo. Am J Anat 188, 109–120.
178. Bogers AJ, Gittenberger-de Groot AC, Poelmann RE, *et al.* (1989) Development of the origin of the coronary arteries, a matter of ingrowth or outgrowth? Anat Embryol (Berl) 180, 437–441.
179. Waldo KL, Kumiski DH, Kirby ML. (1994) Association of the cardiac neural crest with development of the coronary arteries in the chick embryo. Anat Rec 239, 315–331.
180. Drake CJ, Hungerford JE, Little CD. (1998) Morphogenesis of the first blood vessels. Ann N Y Acad Sci 857, 155–179.
181. Waldo K, Kirby M. (1998) Development of the great arteries. In: de la Cruz MV, Markwald RR, editors. *Living Morphogenesis of the Heart*. Boston, MA: Birkhauser. pp. 187–217.
182. Hungerford JE, Little CD. (1999) Developmental biology of the vascular smooth muscle cell: building a multilayered vessel wall. J Vasc Res 36, 2–27.
183. Hungerford JE, Owens GK, Argraves WS, *et al.* (1996) Development of the aortic vessel wall as defined by vascular smooth muscle and extracellular matrix markers. Dev Biol 178, 375–392.
184. Takahashi Y, Imanaka T, Takano T. (1996) Spatial and temporal pattern of smooth muscle cell differentiation during development of the vascular system in the mouse embryo. Anat Embryol (Berl) 194, 515–526.
185. Suri C, Yancopolous GD. (1999) Growth factors in vascular morphogenesis: insights from gene knockout studies in mice. In: Little CD, Mironov V, Sage H, editors. *Vascular Morphogenesis: In Vivo, In Vitro, In Mente*. Boston, MA: Birkhauser. pp. 65–72.
186. Kuo CT, Veselits ML, Barton KP, *et al.* (1997) The LKLF transcription factor is required for normal tunica media formation and blood vessel stabilization during murine embryogenesis. Genes Dev 11, 2996–3006.
187. Winnier GE, Kume T, Deng K, *et al*. (1999) Roles for the winged helix transcription factors MF1 and MFH1 in cardiovascular development revealed by nonallelic noncomplementation of null alleles. Dev Biol 213, 418–431.
188. Douglas YL, Mahtab EA, Jongbloed MR, *et al.* (2009) Pulmonary vein, dorsal atrial wall and atrial septum abnormalities in podoplanin knockout mice with disturbed posterior heart field contribution. Pediatric Res 65, 27–32.
189. Evans HM. (1909) On the development of the aortae, cardinal and umbilical veins, and other blood vessels of vertebrate embryos from capillaries. Anat Rec 3, 498.
190. Larsen WJ. (1993) *Human Embryology*. New York, NY: Churchill Livingston.
191. McClure CFW, Butler EG. (1925) The development of the vena cava inferior in man. Am J Anat 35, 331–383.